Math. Model. Nat. Phenom. 15 (2020) 45
https://doi.org/10.1051/mmnp/2020001

Mathematical Modelling of Natural Phenomena
www.mmnp-journal.org

EFFECTS OF DELAYED IMMUNE-ACTIVATION IN THE DYNAMICS OF TUMOR-IMMUNE INTERACTIONS

Parthasakha Das*, Pritha Das and Samhita Das

Abstract. This article presents the impact of distributed and discrete delays that emerge in the formulation of a mathematical model of the human immunological system describing the interactions of effector cells (ECs), tumor cells (TCs) and helper T-cells (HTCs). We investigate the stability of equilibria and the commencement of sustained oscillations after Hopf-bifurcation. Moreover, based on the center manifold theorem and normal form theory, the expression for direction and stability of Hopf-bifurcation occurring at tumor presence equilibrium point of the system has been derived explicitly. The effect of distributed delay involved in immune-activation on the system dynamics of the tumor is demonstrated. Numerical simulations are also illustrated for elucidating the change of dynamic behavior by varying system parameters.

Mathematics Subject Classification. 97M60, 37C75, 65P30.

Received May 11, 2019. Accepted January 26, 2020.

1. Biological background and motivation

The word "cancer or malignant tumor" is still an enigma and indicates a wide family of high-mortality pathological mechanism in terms of its rapid growth, cellular proliferation as well as deadly impact. According to the American cancer report 2018 [1], more than 15.5 million Americans are suffering from cancer which is the second-largest common cause of death in the USA only. The cellular phenomena of tumor growth are quite complicated and not well understood. The interaction of tumor cells with immune cells and helper T-cells (HTCs) play a vital role to control cancer proliferation. The immune response is activated when the tumor cells (TCs) are recognized [10]. Humoral immunity and cell-mediated immunity are two types of innate immunity that are mediated by antibodies, secreted by B-lymphocytes and T-lymphocytes, respectively. T-lymphocytes rearrange peptide on cell receptor and B-lymphocytes secrete antibodies like cytokines in order to fight against tumor progression. Cytotoxic-T lymphocytes (CTL), macrophages, regulatory cells, and natural killer cells are treated as effector cells. Helper T cells are activated by macrophages and dendrite cells which are observed in all tissues and are circulated in the blood. Helper T-cells help the immune system to increase the activity by secreting cytokines interleukin-2 (known as part of cytokines) to annihilate more and more tumor cells. Indeed, effector cells and helper T-cells are not activated instantaneously but experience a time-lag factor.

Keywords and phrases: Tumor-immune system interactions, delay differential equations, immune-activation distributed delay, Hopf-bifurcation.

Department of Mathematics, Indian Institute of Engineering Science and Technology, Shibpur Howrah, West Bengal, India.

* Corresponding author. parthasakha87das@gmail.com

A summary of significant works of tumor-immune system(T-IS) interaction can be obtained in [2, 3]. In 1994 Kuznetsov *et al.* [30] proposed and studied a mathematical model of a cell-mediated tumor population. The main difference from other models is that it takes into account the percolation of tumor cells (TCs) by effector cells (ECs) as well as inactivation of effector cells. Generalized Kuznetsov model was studied by Kirshner and Panetta [29] to describe the dynamics of interactions between the TCs, ECs, and IL-2. They incorporated adoptive cellular immunotherapy to portray short term oscillations in tumor growth level and also long term tumor relapse. Zhange *et al.* proposed a model which generates periodic and chaotic oscillations in T-IS interaction [7]. De Pills and Radunskaya suggested a model regenerating asynchronous tumor-immune resistance through drug therapy known as Jeff's phenomena [16]. Forys studied Marchuk's model of the immune system for chronic state [22]. Interaction between cancerous cell and micro-environment introducing complex phenomena was discussed in [15, 24]. Banerjee *et al.* emphasized on delay-induced malignant tumor growth and control [4]. Chaotic cancer model also revealed a new approach of research in tumor growth before and after treatment [14].

Incorporating time-lag in T-IS interaction for molecule production, proliferation, differentiation and transportation of cells *etc.* is essential in mathematical model [5, 33] and it influences the dynamics of the physiological system [13, 32]. The study on dynamics of T-IS interaction with discrete delay has been noteworthy interest for a long time [6, 17, 19, 21, 23, 34, 36]. Ruan *et al.* [7] investigated tumor-immune interactions with different discrete delay and established asymptotic stability below some threshold value of delay and Hopf bifurcation at its critical value. Zhang *et al.* studied a model with three delays which results in periodic and chaotic oscillations in tumor-immune system [7].

Recently, distributed delays are considered in cancer-immune system [32]. Some of the researchers studied how the distributed delays affect the dynamics of the system differently from discrete delay [20]. Signal transmission during cellular phenomena can be described by a sequence of linear equation with distributed delay. Immune response is no longer instantaneous and is continuous in nature. With distributed delay, it is easier to shorten the oscillation than with a discrete delay due to negative feedback on the system [11]. A non-negative bounded delay kernel $K(.)$(say) is defined on $[0, \infty)$ is considered which reflects the influence of past states on current dynamics [12].

Dong *et al.* proposed a model on helper T-cells in immune system [17]. Again Dong *et al.* introduced delay kernel as immune-activation in HTCs without taking into account the stimulation of TCs in the presence of ECs along with discrete delays [38]. Helper T-cells do not kill the cancer cell, instead, they continuously help activated immune-effector cell such as cytotoxic T-cells to kill target cell and also help stimulated B-lymphocyte to secrete antibodies and macrophages to kill ingested microbes. Furthermore, effector cells cannot defend the infected target cells without helper-T cells.

Encouraged by the studies briefly outlined above, in this paper, we explore the work of Dong *et al.* [18] by introducing immune-activation delay kernel as an infinite distributed delay for enhancing the continuous stimulation of HTCs. We are interested not only in investigating the model system describing possible phenomena quite exhaustively at the cell level but also in tissue level. Our aim is to study the effect of interaction rate of ECs with TCs, interaction rate of HTCs with TCs and also effect at mean delay which represents the strength of immune activation delay to boost the immunity of HTCs in the dynamics of the system.

The organization of this paper is as follows: Section 2 is devoted to the preliminary description of the delay differential equation governing the interactions between TCs, ECs, and HTCs. In Section 3, the qualitative and analytical study of the system is illustrated which includes positivity of the system, boundedness of the solutions, stability analysis of meaningful biological equilibrium point. We also investigated the existence of Hopf-bifurcation with respect to key parameters. In Section 4 the direction and stability of Hopf-bifurcation with respect to interaction delay is discussed. In Section 5 we carried out extensive numerical simulations to validate our analytical findings. Finally, Section 6 ends with concluding remarks about the key findings of the problem.

2. Mathematical model and preliminaries

It is known that instead of directly killing cancer cell, the helper-T cell help to activate immune-effector cell such as cytotoxic T-cells to attack cancer cell and also stimulate B-lymphocyte to secrete antibodies. As the overall process does not happen instantaneously, the time-lag is needed to make more realistic. Here, we consider the continuous delay kernel on helper-T cells while stimulating effector cells. The delay distribution equation with Gamma type kernel is more appropriate from the aspect of mathematical modeling and analytical tractability. For this purpose, we take Gamma distribution delay kernel as follows, $G_k(t) = \frac{\zeta^{k+1}t^k e^{-\zeta t}}{k}, k = 0, 1, 2...$ where, $\zeta > 0$ indicates the strength of decay of helper-T cells of past states. If $k = 0$, then $G(t) = \zeta e^{-\zeta t}$ describes the weak kernel indicating the maximum weighted response of growth rate in current cell density, *i.e.*, past cell density have decreasing effects. In the contrast, if $k = 1$,then $G(t) = \zeta^2 te^{-\zeta t}$ describes strong kernel indicating the maximum influence on growth response past time. Here, we consider only the weak kernel in our study. Since delay kernel belongs to a family of probability distribution, we consider cell cycle time of helper-T cell positive and $H(t) \geq 0, \forall t \in [0, \infty$ and $\int_0^\infty H(t)\mathrm{d}t = 1$. To apply the Gamma distribution delay kernel on helper-T cells, we define the integro-differential equation

$$K(t) = \int_{-\infty}^{t} le^{-l(t-s)}H(s)\mathrm{d}s, \quad i.e, \quad K(t) = \int_0^t le^{-lv}H(t-v)\mathrm{d}s,$$

where, $l > 0$. le^{-lv} is weight function for $H(t - v)$ and monotonically increasing with respect to v. Whenever l is small, immune activation is considered previous time $(t - v)$ depending on densities of HTCs, similarly when l is large, t takes present time. The present tumor-immune system interaction model is a modification of a model proposed by Dong *et al.* [18]. So, the delay kernel function as immune activation continuous delay is incorporated in the proliferation of effector-cells (ECs) which is stimulated by helper-T cells (HTCs). The following system of DDEs are given

$$\begin{aligned}
\frac{\mathrm{d}T(t)}{\mathrm{d}t} &= aT(t)(1 - mT(t)) - nE(t)T(t)\\
\frac{\mathrm{d}E(t)}{\mathrm{d}t} &= s_1 + k_1T(t - \tau_1)E(t - \tau_1) - d_1E(t) + pE(t)K(t)\\
\frac{\mathrm{d}H(t)}{\mathrm{d}t} &= s_2 + k_2T(t - \tau_2)H(t - \tau_2) - d_2H(t)\\
\frac{\mathrm{d}K(t)}{\mathrm{d}t} &= lH(t) - lK(t),
\end{aligned} \tag{2.1}$$

where $T(t), E(t)$ and $H(t)$ represent the densities of tumor-cells (TCs), effector-cells (ECs) and helper-T cells (HTCs) respectively. The first equation represents the rate of change of TCs densities, the first term of which describes the logistic type growth of TCs, a is the intrinsic growth rate and m^{-1} is maximal cell burden or carrying capacity. The second term corresponds to the inhibition of immune ECs due to the presence of TCs at a rate of n. The second equation corresponds to proliferation enhancement rate of ECs, where the first term represents a constant flow at a rate of s_1 of mature ECs into the region of TCs localization. The second term indicates competition between TCs and ECs, where k_1 is the stimulation rate of ECs lysed and TCs debris. The third term represents ECs natural death with an average half-life $1/d_1$. The fourth term describes the stimulation of ECs with a rate of p by kernel-based HTCs $K(t)$. The third equation represents the rate of change of HTCs, where the first term represents the birth of HTCs, the second term describes stimulation rate of HTCs at k_2 in the localization of tumor-specific antigens and last term represents the HTCs natural death with average half-life $1/d_2$. The fourth equation represents the rate of $K(t)$; where the first term describes the increase of HTCs. The second term represents a loss of $K(t)$ with a strength of l. It is assumed that all parameter value are positive. Figure 1 illustrates the interactions between Tumor-cells(TCs), Effector-cells(ECs) and Helper T-cells(HTCs) with their cellular environment.

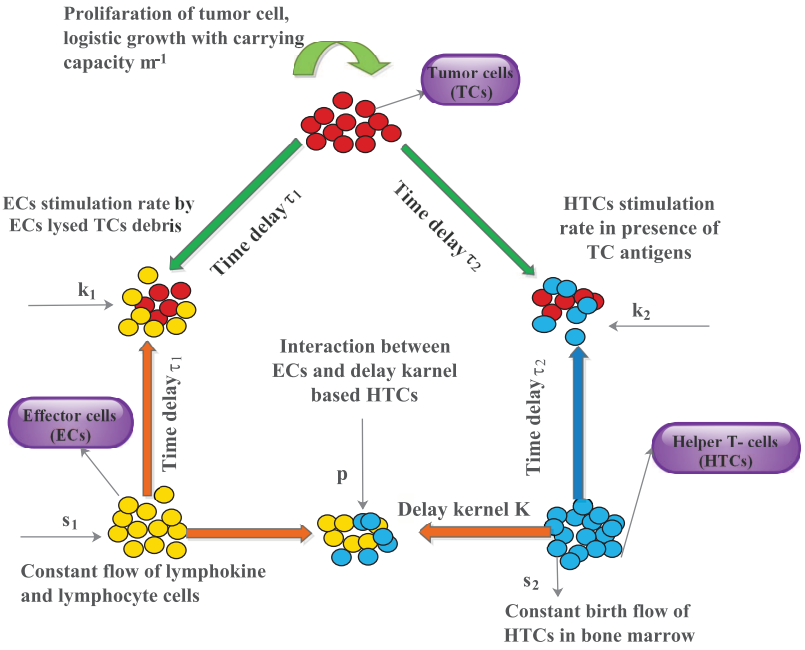

FIGURE 1. The schematic representation of the interactions between Tumor-cells (TCs), Effector-cells (ECs) and Helper T-cells (HTCs).

For the sake of simplicity, we non-dimensionalize model system (2.1) by using the following transformation: $x = \frac{T}{T_0}$, $y = \frac{E}{E_0}$, $z = \frac{H}{H_0}$, $g = \frac{K}{T_0}$, $\nu = nT_0t$, $\alpha = \frac{a}{nT_0}$, $\beta = mT_0$, $\omega_1 = \frac{s_1}{nT_0E_0}$, $\mu_1 = \frac{k_1}{n}$, $r_1 = \frac{d_1}{n}$, $\eta = \frac{p}{n}$, $\omega_2 = \frac{s_2}{nT_0H_0}$, $\mu_2 = \frac{k_2}{n}$, $r_2 = \frac{d_2}{n}$, $b = \frac{1}{nT_0}$, $\overline{\tau}_1 = nT_0\tau_1$, $\overline{\tau}_2 = nT_0\tau_2$.

We take $T_0 = E_0 = H_0 = 10^6$ cells/cm^3 [18, 30] for the improvement of numerical performance. We also consider $\overline{\tau} = \tau$ and replace ν by t. Hence, we get the following dimensionless model equations

$$\begin{aligned}
\frac{\mathrm{d}x(t)}{\mathrm{d}t} &= \alpha x(t)(1-\beta x(t)) - x(t)y(t)\\
\frac{\mathrm{d}y(t)}{\mathrm{d}t} &= \omega_1 + \mu_1 x(t-\tau_1)y(t-\tau_1) - r_1 y(t) + \eta y(t)g(t)\\
\frac{\mathrm{d}z(t)}{\mathrm{d}t} &= \omega_2 + \mu_2 x(t-\tau_2)z(t-\tau_2) - r_2 z(t)\\
\frac{\mathrm{d}g(t)}{\mathrm{d}t} &= bz(t) - bg(t)
\end{aligned} \tag{2.2}$$

with initial conditions $\phi = (\phi_1, \phi_2, \phi_3, \phi_4)$, defined in the space

$$\mathbb{C}_+ = \{\phi \in \mathbb{C}([-\tau, 0], \mathbb{R}^4_+) : x(\xi) = \phi_1(\xi), y(\xi) = \phi_2(\xi), z(\xi) = \phi_3(\xi), g(\xi) = \phi_4(\xi)\}, \tag{2.3}$$

where $\tau = max\{\tau_1, \tau_2\}\phi_i(\xi) \geq 0, i = 1, 2, 3, 4, \xi \in [-\tau, 0]$ and $\mathbb{C}$ is Banach space of continuous functions. $\phi : [-\tau, 0] \to \mathbb{R}^4_+$, with suitable sub-norm, and $\mathbb{R}^4_+ = \{(x, y, z, g) : x \geq 0, y \geq 0, z \geq, g \geq 0\}$.

3. The qualitative analysis of the model

3.1. Positive invariance

Theorem 3.1. *Every solution of the model system(2.2) with initial condition $\phi_1, \phi_2, \phi_3, \phi_4$ are given in (2.3) defined on $[-\tau, 0]$ remains positive for all finite time $t > 0$.*

Consider the model system (2.2) in the vector form $F = (x, y, z, g)^T \in \mathbb{R}^4_+$ and

$$F(Y) = \begin{pmatrix} F_1(Y) \\ F_2(Y) \\ F_3(Y) \\ F_4(Y) \end{pmatrix} = \begin{pmatrix} \alpha x(t)(1-\beta x(t)) - x(t)y(t) \\ \omega_1 + \mu_1 x(t-\tau_1)y(t-\tau_1) - r_1 y(t) + \eta y(t)g(t) \\ \omega_2 + \mu_2 x(t-\tau_2)z(t-\tau_2) - r_2 z(t) \\ bz(t) - bg(t), \end{pmatrix}$$

where the mapping $F : \mathbb{C}_+ \to \mathbb{R}^4_+$ and $F \in \mathbb{C}^\infty(\mathbb{R}^4_+)$, then the system can be written as

$$\dot{Y} = F(Y_t) \tag{3.1}$$

with initial condition $Y_t(\xi) = Y(t+\xi), \xi \in [-\tau, 0]$. Considering (3.1) and choosing $Y(\xi) \in \mathbb{C}_+$ such that $Y_i = 0$. We get $F_i(Y)|_{Y_i(t)} = F_i(0) \geq 0, \quad \forall \quad Y_t \in \mathbb{C}_+, \quad i = 1, 2, 3, 4$. Using lemma by Yang *et al.* [37], for any solution of $\dot{Y} = F(Y_t)$ with $Y_t(\xi) \in \mathbb{C}_+$ and $Y(t) = Y(t, Y(0))$, we get $Y(t) \in \mathbb{R}^4_+, \quad \forall \quad t \geq 0$ *i.e.*, it remains non-negative throughout whole region $\mathbb{R}^4_+$.

3.2. Boundedness

The model equation (2.2) is a Lipchitz continuous function, which implies that there exists a unique solution of (2.2) with initial condition $(\phi_1, \phi_2, \phi_3, \phi_4)$. By using Theorem 3.1, we obtain $\frac{\mathrm{d}x}{\mathrm{d}t} \leq \alpha x(t)(1-\beta x(t))$, Using standard Kamke's comparison theory, it follows that $\lim\limits_{t\to\infty} sup \;\; x(t) \leq \frac{1}{\beta}, \;\; x(t) \leq max\{T_0, \frac{1}{\beta}\}$.
Again, from second equation of model system (2.2)

$$y(t) = e^{-r_1 t}[y(0) + \frac{\omega_1}{r_1}e^{r_1 t} + \int_0^t (\eta y(t)g(t) + \mu_1 x(t-\tau_1)y(t-\tau_1)e^{r_1 t}\mathrm{d}s)].$$

Assuming that $\sup g(t) = g_\theta > 0$, say. Since, $e^{-r_1 t} \in (0, 1], \;\; x(t) \leq \frac{1}{\beta}$, we have

$$y(t) \leq [y(0) + \tfrac{\omega_1}{r_1}e^{r_1 t} + \textstyle\int_0^t (\eta g_\theta + \frac{\mu_1}{\beta})e^{r_1 s}\mathrm{d}s].$$

We use generalized Gronwall's Lemma [9]

$$y(t) \leq [y(0) + \frac{\omega_1}{r_1}e^{r_1 t} + \int_0^t [(\eta M_1 + \frac{\mu_1}{\beta})e^{r_1(\tau_1+s)}(y(0) + \frac{\omega_1}{r_1}e^{r_1 t})e^{(\int_s^t e^{r_1(\tau_1+\xi)}d\xi)}]\mathrm{d}s = M_1(\text{say}).$$

Similarly, we get

$$z(t) \leq z(0) + \frac{\omega_2}{r_2}e^{r_2 t} + \int_0^t [(\eta g_\theta + \frac{\mu_2}{\beta})e^{r_2(\tau_2+s)}(z(0) + \frac{\omega_2}{r_2}e^{r_2 t})e^{(\int_s^t e^{r_2(\tau_2+\xi)}d\xi)}]\mathrm{d}s = M_2(\text{say}),$$

and also, we obtain

$$g(t) \leq g(0) + \frac{\omega_2}{r_2}e^{r_2 t} + \int_0^t [(\eta g_\theta + \frac{\mu_2}{\beta})e^{r_1 t}(g(0) + \frac{\omega_2}{r_2}e^{r_2 t})e^{(\int_s^t e^{r_2\xi}d\xi)}]\mathrm{d}s = M_3(\text{say}).$$

Here, M_1, M_2, M_3 are non-negative. Now, $g(t) \leq max\{g_\theta, M_3\}$. From above, it is clear that $x(t), y(t), z(t), g(t)$ are bounded on $\in \mathbb{R}^4_+, \quad \forall \quad t \geq 0$.

3.3. Equilibria

The model system (2.2) has following biologically feasible equilibrium points:

i) tumor-free equilibrium $E_0 = (x_0, y_0, z_0, g_0) = (0, \frac{\omega_1 r_2}{r_1 r_2 - \eta\omega_2}, \frac{\omega_2}{r_2}, \frac{\omega_2}{r_2})$
ii) tumor-presence equilibrium $E_1 = (x_1, y_1, z_1, g_1) = (x_1, \alpha(1-\beta x_1), \frac{\omega_2}{r_2 - \mu_2 x_1}, \frac{\omega_2}{r_2 - \mu_2 x_1})$.

E_0 exists if $\eta < \frac{r_1 r_2}{\omega_2} \equiv \eta_0$ holds.

Making $x_1 \neq 0$ and removing y_1 and z_1 from steady state equations of the system (2.2), we get the equation in x_1 for the existence of tumor presence equilibrium as

$$F(x) = \alpha\beta\mu_1\mu_2 x_1^3 - \alpha\mu_1(\beta r_2 + \mu_2)x_1^2 + (\alpha\mu_1 r_2 - \mu_2\omega_1 + \alpha\beta r_1 - r_1\eta_1\omega_2)x_1 + \omega_1 r_2 - r_1 r_2\alpha + \eta\alpha\omega_2 = 0$$

Now $\lim_{x_1 \to \infty} F(x_1) = +\infty$. It can be mentioned that the equation x_1 has atleast on positive real root if $\omega_1 r_2 - r_1 r_2\alpha + \eta\alpha\omega_2 < 0$, *i.e.*, $\eta < \frac{r_1 r_2}{\omega_2} - \frac{\omega_1 r_2}{\alpha\omega_2} \equiv \eta_1$.

Remark 3.2. The system (2.2) has atleast one tumour-presence equilibrium E_1 when $0 < \eta < \eta_1$.

3.4. Stability analysis

In order to study the local dynamics of the system (2.2), the Jacobian matrix J_{E^*} of the system (2.2) about positive equilibrium points $E^*(x^*, y^*, z^*, g^*)$ is given by

$$J_E = \det \begin{pmatrix} \alpha - 2\alpha\beta x^* - y^* - \lambda & -x^* & 0 & 0 \\ \mu_1 y^* e^{-\lambda\tau_1} & -r_1 + \eta g^* + \mu_1 x^* e^{-\lambda\tau_1} - \lambda & 0 & \eta y^* \\ \mu_2 y^* e^{-\lambda\tau_2} & 0 & -r_2 + \eta g^* + \mu_2 x^* e^{-\lambda\tau_2} - \lambda & 0 \\ 0 & 0 & b & -b - \lambda \end{pmatrix}$$

and corresponding characteristic equation is,

$$J_{E^*}(\lambda, \tau_1, \tau_2) = q_0(\lambda) + q_1(\lambda)e^{-\lambda\tau_1} + q_2(\lambda)e^{-\lambda\tau_2} + q_{12}(\lambda)e^{-\lambda(\tau_1+\tau_2)} = 0, \tag{3.2}$$

where λ is eigenvalue and

$$\begin{aligned} q_0(\lambda) &= -(\alpha - 2\alpha\beta x^* - y^* - \lambda)(b+\lambda)(r_1 + \lambda - \eta g^*)(r_2 + \lambda) \\ q_1(\lambda) &= (\alpha - 2\alpha\beta x^* - y^* - \lambda)(b+\lambda)(r_2 + \lambda)\mu_1 x^* + (b+\lambda)(r_2+\lambda)\mu_1 x^* y^* \\ q_2(\lambda) &= (\alpha - 2\alpha\beta x^* - y^* - \lambda)(b+\lambda)(r_1 + \lambda - \eta g^*)\mu_2 x^* + \eta b x^* y^* z^* \mu_2 \\ q_{12}(\lambda) &= -(\alpha - 2\alpha\beta x^* - y^* - \lambda)(b+\lambda)\mu_1\mu_2 x^{*2} - x^{*2} y^* \mu_1\mu_2(b+\lambda). \end{aligned}$$

Theorem 3.3. *The tumor-free equilibrium point E_0 of the model system (2.2) is locally asymptotically stable if $\eta_1 < \eta < \eta_0$ for any $\tau_1, \tau_2 > 0$.*

Proof. The characteristic equation (3.2) at $E_0 = (0, y_0, z_0, g_0)$ becomes

$$(b+\lambda)(r_2+\lambda)(\alpha - y_0 - \lambda)(r_1 + \lambda - \eta g_0) = 0.$$

The eigenvalues of J_{E_0} are $\lambda_1^0 = -b < 0, \lambda_2^0 = -r_2 < 0, \lambda_3^0 = \alpha - \frac{\omega_1 r_2}{r_1 r_2 - \eta\omega_2}$, $\lambda_4^0 = \eta\frac{\omega_1}{r_2} - r_1 < 0$. so, E_0 locally asymptotically stable when $\lambda_3^0 = \alpha - \frac{\omega_1 r_2}{r_1 r_2 - \eta\omega_2} < 0$, *i.e.*, $\eta_1 < \eta < \eta_0$. □

Now we investigate the local stability of tumor-presence equilibrium with influence of discrete time delay τ_1, τ_2.

Case I: $\tau_1 = \tau_2 = 0$.

The characteristic equation (3.2) becomes

$$J_{E^*}(\lambda) \equiv q_0(\lambda) + q_1(\lambda) + q_2(\lambda) + q_{12}(\lambda) = 0. \tag{3.3}$$

The characteristic equation at $E_1(x_1, y_1, z_1, g_1)$ is given by

$$\lambda^4 + A_3\lambda^3 + A_2\lambda^2 + A_1\lambda + A_0 = 0, \tag{3.4}$$

where,

$$\begin{aligned}
A_3 &= b + \alpha\beta x_1 + \mu_1 x_1 + \frac{\omega_1}{y_1} + \frac{\omega_2}{z_1} \\
A_2 &= \alpha\beta x_1(1 + \mu_1 + b + \frac{\omega_2}{z_1}) + b(\mu_1 x_1 + \frac{\omega_2}{z_1} + \frac{\omega_1}{y_1}) + \frac{\omega_2}{z_1}\frac{\omega_1}{y_1} \\
A_1 &= \alpha\beta x_1(bx_1^2\mu_1\mu_2 + bx_1(\mu_2\frac{\omega_1}{y_1} + \mu_1\frac{\omega_2}{z_1}) - \mu_2 x_1) + \mu_1 x_1 y_1\frac{\omega_2}{z_1} \\
A_0 &= b(\eta\mu_2 x_1 y_1 z_1 - \mu_1\mu_2 x_1^2 y_1 + \alpha\beta x_1\frac{\omega_2}{z_1}\frac{\omega_1}{y_1}).
\end{aligned}$$

By well-known Routh-Hurwitz criterion, all the roots of equation (3.4) have negative real parts if and only if

$$A_3 > 0, A_3A_2 - A_1 > 0, (A_3A_2 - A_1)A_1 - A_3^2A_0 > 0 \text{ and } [(A_3A_2 - A_1)A_1 - A_3^2A_0]A_0 > 0. \tag{3.5}$$

It is clear that the tumor-presence equilibrium is locally asymptotically stable if the condition (3.5) holds.

Case II: $\tau_1 > 0, \tau_2 = 0$.

The characteristic equation (3.2) becomes

$$J_{E^*}(\lambda, \tau_1) \equiv q_0(\lambda) + q_2(\lambda) + (q_1(\lambda) + q_{12}(\lambda))e^{-\lambda\tau_1} = 0. \tag{3.6}$$

The characteristic equation at $E_1(x_1, y_1, z_1, g_1)$ is given by

$$\begin{aligned}
\lambda^4 + a_3\lambda^3 + a_2\lambda^2 + a_1\lambda + a_0 + (b_3\lambda^3 + b_2\lambda^2 + b_1\lambda + b_0)e^{-\lambda\tau_1} &= 0 \\
D(\lambda) + Q(\lambda)e^{-\lambda\tau_1} &= 0,
\end{aligned} \tag{3.7}$$

where,

$$\begin{aligned}
D(\lambda) &= \lambda^4 + a_3\lambda^3 + a_2\lambda^2 + a_1\lambda + a_0 \\
Q(\lambda) &= b_3\lambda^3 + b_2\lambda^2 + b_1\lambda + b_0 \\
a_3 &= (r_1 + r_2 - \eta g_1) + (b + \alpha\beta x_1) - \mu_1 x_1 \\
a_2 &= r_2(r_1 - \eta g_1) + (b + \alpha\beta x_1)(r_1 + r_2 - \eta g_1) + b\alpha\beta x_1 - \mu_2 x_1(r_1 - \eta g_1 + b + \alpha\beta x_1) \\
a_1 &= r_2(r_1 - \eta g_1)(b + \alpha\beta x_1) + b\alpha\beta x_1(r_1 + r_2 - \eta g_1) - \mu_2 x_1(b + \alpha\beta x_1)(r_1 - \eta g_1) - b\mu_2\alpha\beta x_1^2 \\
a_0 &= b\alpha\beta r_2 x_1(r_1 - \eta g_1) - b\mu_2\alpha\beta x_1^2(r_1 - \eta g_1) + b\eta x_1 y_1 z_1\mu_2
\end{aligned}$$

and

$$b_3 = -\mu_2 x_1$$

$$
\begin{aligned}
b_2 &= -\mu_2 x_1(r_1 - \eta g_1 + b + \alpha\beta x_1)\\
b_1 &= -\mu_2 x_1[(b + \alpha\beta x_1)(r_1 - \eta g_1) + b\alpha\beta x_1]\\
b_0 &= -b\mu_2\alpha\beta x_1^2(r_1 - \eta g_1) + b\eta x_1 y_1 z_1 \mu_2.
\end{aligned}
$$

It can be mentioned that the characteristic equation (3.7) containing λ, τ has infinitely many eigenvalues. So, Routh-Hurwitz criterion is unable to investigate the locally asymptotical stability of equation (3.7). The local asymptotical stability of E_1 occurs if all roots of equation (3.7) have negative real parts, otherwise, stability is lost if a purely complex root crosses the imaginary axis from left to right. To investigate the sign of the real part of the roots, we use analytic arguments of Ruan and Wei [35]. We substitute $\lambda = i\theta$ into the equation (3.7) to get periodic solutions which are significant in tumor dynamics. Separating the real and imaginary parts, we obtain the following transcendental equations

$$
\begin{aligned}
\theta^4 - a_2\theta^2 + a_0 &= (b_2\theta^2 - b_0)\cos\theta\tau_1 + (b_3\theta^3 - b_1\theta)\sin\theta\tau_1\\
a_3\theta^3 - a_1\theta &= (b_1\theta - b_3\theta^3)\cos\theta\tau_1 - (b_0 - b_2\theta^2)\sin\theta\tau_1.
\end{aligned} \tag{3.8}
$$

Squaring and adding both the equations of (3.7), we have

$$
(\theta^4 - a_2\theta^2 + a_0)^2 + (a_3\theta^3 - a_1\theta)^2 = (b_0 - b_2\theta^2)^2 + (b_1\theta - b_3\theta^3)^2
$$

which implies

$$
\theta^8 + e_3\theta^6 + e_2\theta^4 + e_1\theta^2 + e_0 = 0, \tag{3.9}
$$

where,

$$
\begin{aligned}
e_3 &= a_2^2 - b_3^2 - 2a_2\\
e_2 &= a_2^2 + 2a_0 - 2a_1a_3 - b_2^2 + 2b_1b_2\\
e_1 &= a_1^2 - 2a_0a_2 + 2b_0b_2 + b_1^2\\
e_0 &= a_0^2 - b_0^2.
\end{aligned}
$$

Denote $v = \theta^2$. Then simplified version of equation (3.9) is

$$
F(v) = v^4 + e_3v^3 + e_2v^2 + e_1v + e_0. \tag{3.10}
$$

Since, $\lim_{v\to\infty} F(v) = +\infty$. so, it can be concluded that the equation (3.10) has atleast one positive real root, if $e_0 < 0$, $i.e.,\ \ a_0^2 - b_0^2 < 0$. Without loss of generality, we assume that equation (3.10) has four positive roots, which are defined by v_1, v_2, v_3 and v_4 respectively. Then equation (3.10) has four positive roots $\theta_k = \sqrt{v_k}, k = 1, 2, 3, 4$. Eliminating $\sin\theta\tau_1$ from equation (3.8) we get the expression for time delay τ_1 as

$$
\tau_{1,k}^j = \frac{1}{\theta_k}\cos^{-1}\left\{\frac{(b_2 - a_3b_3)\theta_k^6 + (a_3b_1 - a_2b_2 + a_1b_3 - b_0)\theta_k^4 + (a_2b_0 + a_0b_2 - a_1b_1)\theta_k^2 - a_0b_0}{(b_2\theta_k^2 - b_0)^2 + (b_3\theta_k^3 - b_1\theta_k)^2}\right\} + \frac{2k\pi}{\theta_k} \tag{3.11}
$$

where $k = 1, 2, 3, 4;\ \ j = 0, 1, 3.....$, and $\pm i\theta_k$ is pair of pure imaginary roots of equation (3.9) with $\tau_{1,k}^j$ given by (3.11). We define

$$
\tau_1^* = \tau_{1,k_0}^0 \min_{k\in\{1,2,3,4\}}\left\{\tau_{1,k}^{(0)}\right\}, \qquad \theta^* = \theta_{k_0}. \tag{3.12}
$$

Case III: $\tau_1 = 0, \tau_2 > 0$.
The characteristic equation (3.2) becomes

$$J_{E^*}(\lambda, \tau_2) \equiv q_0(\lambda) + q_1(\lambda) + (q_2(\lambda) + q_{12}(\lambda))e^{-\lambda\tau_2} = 0. \tag{3.13}$$

The characteristic equation at $E_1(x_1, y_1, z_1, g_1)$ is given by

$$\begin{aligned} \lambda^4 + c_3\lambda^3 + c_2\lambda^2 + c_1\lambda + c_0 + (d_3\lambda^3 + d_2\lambda^2 + d_1\lambda + d_0)e^{-\lambda\tau_2} = 0 \\ A(\lambda) + B(\lambda)e^{-\lambda\tau_2} = 0, \end{aligned} \tag{3.14}$$

where,

$$\begin{aligned} A(\lambda) &= \lambda^4 + c_3\lambda^3 + c_2\lambda^2 + c_1\lambda + c_0 \\ B(\lambda) &= d_3\lambda^3 + d_2\lambda^2 + d_1\lambda + d_0 \\ c_3 &= (b + r_2) - (\alpha - 2\alpha\beta x_1 - y_1 + r_1 - \eta g_1) - \mu_2 x_1 \\ c_2 &= br_2 - (\alpha - 2\alpha\beta x_1 - y_1)(r_1 - \eta g_1) - (b + r_2)(\alpha - 2\alpha\beta x_1 - y_1 + r_1 - \eta g_1 - \mu_2 x_1) - b\mu_2 x_1 \\ c_1 &= (\alpha - 2\alpha\beta x_1 - y_1)(r_1 - \eta g_1)(b + r_2 - br_2 + \mu_2 x_1) + (\alpha - 2\alpha\beta x_1 - y_1 - r_1 - \eta g_1)(\mu_2 b x_1 - br_2) \\ c_0 &= (b\mu_2 x_1 - br_2)(\alpha - 2\alpha\beta x_1 - y_1)(r_1 - \eta g_1) - \eta\mu_2 b x_1 y_1 z_1 \end{aligned}$$

and

$$\begin{aligned} d_3 &= -\mu_2 x_1 \\ d_2 &= \mu_2 x_1(\alpha - 2\alpha\beta x_1 - y_1 - b - r_2) - \mu_1 x_1 y_1 + \mu_1\mu_2 x_1^2 \\ d_1 &= \mu_1\mu_2 x^2(b - \alpha + 2\alpha\beta x_1 + y_1) - \mu_2 x_1 br_2 + \mu_2 x_1(b + r_2)(\alpha - 2\alpha\beta x_1 - y_1) - \mu_1 x_1 y_1(b + r_2 + x_1\mu_2) \\ d_0 &= (\mu_2 x_1 + br_2\mu_2 x_1 - b\mu_1\mu_2 x_1^2(\alpha - 2\alpha\beta x_1 - y_1) - \mu_1\mu_2 br_2 x_1 y_1 - b\mu_1\mu_2 x_1^2 y_1. \end{aligned}$$

Now, we put $\lambda = i\phi$ in equation (3.14) and proceed in similar way as (3.8)–(3.10). We obtain the expression for time delay τ_2 as

$$\tau_{2,k}^j = \frac{1}{\phi_k}\cos^{-1}\left\{\frac{(d_2 - c_3 d_3)\phi_k^6 + (c_3 d_1 - c_2 d_2 + c_1 d_3 - d_0)\phi_k^4 + (c_2 d_0 + c_0 d_2 - c_1 d_1)\phi_k^2 - c_0 d_0}{(d_2\phi_k^2 - d_0)^2 + (d_3\phi_k^3 - d_1\phi_k)^2}\right\} + \frac{2k\pi}{\phi_k} \tag{3.15}$$

where $k = 1, 2, 3, 4$; $j = 0, 1, 3.....$, and $\pm i\phi_k$ is pair of pure imaginary roots of equation (3.13) with $\tau_{2,k}^j$ given by (3.15). We define

$$\tau_2^* = \tau_{2,k_0}^0 \min_{k\in\{1,2,3,4\}}\left\{\tau_{2,k}^{(0)}\right\}, \qquad \phi^* = \phi_{k_0}. \tag{3.16}$$

3.4.1. Analysis of Hopf Bifurcation

As pair of purely imaginary roots arise, we need to investigate the Hopf bifurcation analysis [26] in the system (2.2) and verify the transversality condition $\frac{\mathrm{d}(Re\lambda)}{\mathrm{d}\tau_1}|_{\tau_1=\tau_1^*} > 0$ which also preserves the conditions for the existence of periodic solution. We put $\pm i\theta_k$ in characteristic equation (3.7) such that $|D(i\theta_k)| = |Q(i\theta_k)|$,which also gives

set of values of τ_k^j. Our main aim is to study the direction of motion of λ whenever τ_1 varies. Now we calculate

$$\Phi = sign\left[\frac{\mathrm{d}(Re\lambda)}{\mathrm{d}\tau_1}\right]\Big|_{\tau_1=\tau_1^*} = sign\left[Re\left(\frac{\mathrm{d}\lambda}{\mathrm{d}\tau_1}\right)^{-1}\right]\Big|_{\tau_1=\tau_1^*}.$$

Differentiating equation (3.7) with respect to τ_1, we have

$$[4\lambda^3 + 3a_3\lambda^2 + 2a_2\lambda + a_1 + \{(3b_3\lambda^2 + 2b_2\lambda + b_1)e^{-\lambda\tau_1} - \tau_1(b_3\lambda^3 + b_2\lambda^2 + b_1\lambda + b_0)e^{-\lambda\tau_1}\}]\frac{\mathrm{d}\lambda}{\mathrm{d}\tau_1}$$
$$= \lambda(b_3\lambda^3 + b_2\lambda^2 + b_1\lambda + b_0)e^{-\lambda\tau_1},$$

which implies

$$\left(\frac{\mathrm{d}\lambda}{\mathrm{d}\tau_1}\right)^{-1} = -\frac{4\lambda^3 + 3a_3\lambda^2 + 2a_2\lambda + a_1}{\lambda(\lambda^4 + a_3\lambda^3 + a_2\lambda^2 + a_1\lambda + a_0)} + \frac{3b_3\lambda^2 + 2b_2\lambda + b_1}{\lambda(b_3\lambda^3 + b_2\lambda^2 + b_1\lambda + b_0)} - \frac{\tau_1}{\lambda}.$$

Now, evaluating Φ at $\tau_1 = \tau_1^*(i.e., \lambda = i\theta^*)$, we have

$$\begin{aligned}
\Phi &= sign\left\{Re\left[-\frac{4\lambda^3 + 3a_3\lambda^2 + 2a_2\lambda + a_1}{\lambda(\lambda^4 + a_3\lambda^3 + a_2\lambda^2 + a_1\lambda + a_0)} + \frac{3b_3\lambda^2 + 2b_2\lambda + b_1}{\lambda(b_3\lambda^3 + b_2\lambda^2 + b_1\lambda + b_0)} - \frac{\tau_1}{\lambda}\right]_{\lambda=i\theta^*}\right\} \\
&= \frac{4\theta^{*6} + 3(a_2^2 - b_3^2 - 2a_2)\theta^{*4} + 2(a_2^2 + 2a_0 - 2a_1a_3 - b_2^2 + 2b_1b_2)\theta^{*2} + a_1^2 - 2a_0a_2 + 2b_0b_2 + b_1^2}{(b_0 - b_2\theta^{*2})^2 + (b_1\theta^* - b_3\theta^{*3})^2} \\
&= \frac{4\theta^{*6} + 3e_3\theta^{*4} + 2e_2\theta^{*2} + e_1}{(b_0 - b_2\theta^{*2})^2 + (b_1\theta - b_3\theta^{*3})^2} \\
&= \frac{F'(\theta^{*2})}{(b_0 - b_2\theta^{*2})^2 + (b_1\theta - b_3\theta^{*3})^2}.
\end{aligned}$$

Therefore, if $F'(\theta^{*2}) \neq 0$, the transversality condition holds and Hopf bifurcation occurs at $\theta = \theta^*, \tau_1 = \tau_1^*$. Hence, delay based tumor model has a small amplitude periodic solution bifurcating from the tumor free equilibrium point as bifurcating parameter τ_1 crosses critical value $\tau_1 = \tau_1^*$, where τ_1^* is least positive value given by (3.11). Now we summarize the results as a theorem:

Theorem 3.4. *For $\tau_1 > 0, \tau_2 = 0$, assume that the condition (3.7) holds for the model system (2.2) with initial conditions (2.3). If $e_0 < 0$, i.e., $a_0^2 - b_0^2 < 0$.*
Then,

i) the tumor presence equilibrium E_1 is locally asymptotically stable, if $\tau_1 < \tau_1^*$,
ii) the tumor presence equilibrium E_1 is unstable, if $\tau_1 > \tau_1^*$,
iii) the system (2.2) experiences a Hopf-bifurcation around the tumor presence equilibrium E_1 at $\tau_1 = \tau_1^*$,

where,

$$\tau_1^* = \frac{1}{\theta^*}\arccos\frac{(b_2 - a_3b_3)\theta^{*6} + (a_3b_1 - a_2b_2 + a_1b_3 - b_0)\theta^{*4} + (a_2b_0 + a_0b_2 - a_1b_1)\theta^{*2} - a_0b_0}{(b_2\theta^{*2} - b_0)^2 + (b_3\theta^{*3} - b_1\theta^*)^2}. \tag{3.17}$$

In similar way, we can formulate a theorem for time delay τ_2.

Theorem 3.5. *For $\tau_1 = 0, \tau_2 > 0$, assume that the condition (3.14) holds for the model system (2.2) with initial conditions (2.3). If $e_0 < 0$, i.e., $a_0^2 - b_0^2 < 0$.*
Then,

i) the tumor presence equilibrium E_1 is locally asymptotically stable, if $\tau_2 < \tau_2^*$,

ii) the tumor presence equilibrium E_1 is unstable, if $\tau_2 > \tau_2^*$,
iii) the system (2.2) experiences a Hopf-bifurcation around the tumor presence equilibrium E_1 at $\tau_2 = \tau_2^*$,

where,

$$\tau_1^* = \frac{1}{\phi^*}\arccos\frac{(d_2 - c_3d_3)\phi^{*6} + (c_3d_1 - c_2d_2 + c_1d_3 - d_0)\phi^{*4} + (c_2d_0 + c_0d_2 - c_1d_1)\phi^{*2} - c_0d_0}{(d_2\phi^{*2} - d_0)^2 + (d_3\phi^{*3} - d_1\phi^*)^2}. \tag{3.18}$$

Case IV: $\tau_1 > 0, \tau_2 > 0$.
Now, we study the dynamics of tumor-presence equilibrium E_1 of the system in presence of time delays $\tau_1 > 0, \tau_2 > 0$. In order to study the stability of E_1, we need to show that all roots of (3.2) have negative real parts. We consider that (3.2) is initially locally stable for $\tau \in [0, \tau_1^*)$ and also consider τ_2 as a parameter. Ruan and Wei [35] analyzed in which conditions zeros of exponential polynomial have negative real parts.

Theorem 3.6. *If roots of $J_{E^*}(\lambda, \tau_1) = 0$ have negative real parts then there exists $\tau_2 = f(\tau_1) > 0$ which is function of τ_1, such that whenever $\tau_2 \in [0, f(\tau_1))$, roots of $J_{E^*}(\lambda, \tau_1, \tau_2) = 0$ have negative real parts.*

Proof. Consider that $J_{E^*}(\lambda, \tau_1) = 0$ has no roots with non-negative real parts. Hence, $J_{E^*}(\lambda, \tau_1, \tau_2) = 0$ with $\tau_1 > 0, \tau_2 = 0$ contains no root with non-negative real parts. Again, assume that τ_2 is a parameter. As τ_2 varies, it can be shown that $J_{E^*}(\lambda, \tau_1, \tau_2)$ is analytic in λ and sum of multiplicity of all roots of $J_{E^*}(\lambda, \tau_1, \tau_2) = 0$ in right half plane can be altered if zero arrives on or crosses the imaginary axis. Thus, if $J_{E^*}(\lambda, \tau_1, \tau_2) = 0$ with $\tau_2 = 0$ contains no root with non-negative real parts, then there exits $\tau_2^* > (\tau_2^* = f(\tau_1))$ such that all roots of $J_{E^*} = 0$ with $\tau_2 \in [0, \tau_2^*)$ contains negative real parts. □

4. Direction and stability analysis of Hopf bifurcation

From the previous section, we know that the model system (2.2) undergoes Hopf-bifurcation at E_1 under certain conditions. In this section we will study the stability and direction of Hopf-bifurcating periodic solution when the bifurcation parameter τ_1 passes through critical value $\tau_1 = \tau_1^*$ using center manifold reduction of following the ideas of Hassard *et al.* [26]. Now we translate the point $E_1 = (x_1, y_1, z_1, g_1)$ to the origin by using translator $u_1 = x(t) - \overline{x}, u_2 = y(t) - \overline{y}, u_3 = z(t) - \overline{z}, u_1 = x(t) - \overline{x}, u_4 = g(t) - \overline{g}$.
Let $x_i = u_i(\tau t)$ and $\tau = \tau_0 + t$, for simplicity $\tau_0 = \tau_{1,k}^j$, where $k = 1, 2; j = 0, 1, 2, 3$ and $\mu = \mathbb{R}$. Then the system (2.2) can be expressed as a form of functional differential equation(FDE) in $\mathbb{C} = \mathbb{C}([-\tau, 0], \mathbb{R}^4)$,

$$\frac{\mathrm{d}x}{\mathrm{d}t} = L_\mu(x_t) + f(\mu, x_t) \tag{4.1}$$

where $(x_1(t), x_2(t), x_3(t), x_4(t))^T \in \mathbb{R}^4$, $x_t(\nu) = x(\nu + t) \in \mathbb{C}([-\tau_1, 0])$ and $L_\mu : \mathbb{C} \to \mathbb{R}^4$, $F : \mathbb{C} \to \mathbb{R}^4$ are given by

$$L_\mu(\psi) = (\tau_0 + \mu)M_0\psi(0) + (\tau_0 + \mu)M_1\psi(-\tau_1) + (\tau_0 + \mu)M_2\psi(-\tau_2). \tag{4.2}$$

Let $A_0 = \alpha - 2\alpha\beta x_1y_1 - y_1$ and

$$M_0 = \begin{pmatrix} A_0 & -x_1 & 0 & 0 \\ 0 & -r_1 + \eta g_1 & 0 & \eta y_1 \\ 0 & 0 & -r_2 & 0 \\ 0 & 0 & b & -b \end{pmatrix}, M_1 = \begin{pmatrix} 0 & 0 & 0 & 0 \\ \mu_1 y_1 & \mu x_1 & 0 & 0 \\ 0 & 0 & 0 & 0 \\ 0 & 0 & 0 & 0 \end{pmatrix}, M_2 = \begin{pmatrix} 0 & 0 & 0 & 0 \\ 0 & 0 & 0 & 0 \\ \mu_1 z_1 & 0 & \mu_1 x_1 & 0 \\ 0 & 0 & 0 & 0 \end{pmatrix},$$

$$f(\mu, x_t) = (\tau_0 + \mu)\begin{pmatrix} -\alpha\beta\psi_1^2(0) - \psi_1(0)\psi_2(0) \\ \eta\psi_2(0)\psi_4(0) + \mu_1\psi_1(-\tau_1)\psi_2(-\tau_1) \\ \mu_2\psi_1(-\tau_2)\psi_3(-\tau_2). \\ 0 \end{pmatrix} \tag{4.3}$$

By the Riesz representation theorem, there exists a function $\zeta(\nu,\mu)$ of bounded variation for $\nu \in [-\tau_1, 0]$ such that

$$L_\mu(\psi) = \int_{-\tau_1}^{0} \mathrm{d}\zeta(\nu,0)\psi(\nu), \quad \text{and} \quad \psi \in \mathbb{C}([-\tau_1,0],\mathbb{R}). \tag{4.4}$$

Now we may take

$$\zeta(\nu,\mu) = (\tau_0+\mu)(M_0\delta(\nu) + M_1\delta(\nu+\tau_1) + M_2\delta(\nu+\tau_2)) \tag{4.5}$$

where δ is Dirac delta function. Let us define

$$R(\mu)\psi = \begin{cases} \frac{\mathrm{d}\psi(\nu)}{\mathrm{d}\nu} & \text{if } \nu \in [-\tau_1,0] \\ \int_{-\tau_1}^{0} \mathrm{d}\zeta(\mu,s)\psi(s) & \text{if } \nu = 0 \end{cases} \tag{4.6}$$

and

$$Q(\mu)\psi = \begin{cases} 0 & \text{if } \nu \in [-\tau_1,0] \\ f(\mu,\psi) & \text{if } \nu = 0 \end{cases} \tag{4.7}$$

then the system(4.1) is equivalent to

$$\frac{\mathrm{d}x}{\mathrm{d}t} = R(\mu)x_t + Q(\mu)x_t, \tag{4.8}$$

where $x_t(\nu) = x(t+\nu), for \nu \in \mathbb{C}([-\tau_1,0],\mathbb{R}^4)$, now we define

$$R^*(\mu)\chi(s) = \begin{cases} -\frac{\mathrm{d}\chi(s)}{\mathrm{d}s} & \text{if} s \in [0,\tau_1] \\ \int_{-\tau_1}^{0} \mathrm{d}\zeta^T(t,0)\chi(-t) & \text{if} s = 0 \end{cases} \tag{4.9}$$

Again we define a bilinear inner product

$$\langle \psi(s), \chi(\nu)\rangle = \overline{\psi}(0)\chi(0) - \int_{-\tau_1}^{0}\int_{\xi=0}^{\nu} \overline{\psi}(\xi-\nu)\mathrm{d}\zeta(\nu)\chi(\xi)\mathrm{d}\xi, \qquad \zeta(\nu) = [\zeta(\nu,0)]. \tag{4.10}$$

$R(0)$ and R^* are known as adjoint operators. From the previous section, we have $\pm i\tau_0\theta_k$ which are eigenvalues of $R(0)$ as well as of R^*. Now we are interested to evaluate the eigenvectors $R(0)$ and R^*. Let $p(\nu) = (1,\alpha_1,\alpha_2,0)^T e^{i\tau_0\theta_k\nu}$ is eigenvector of $R(0)$ corresponding to $i\tau_0\theta_k$, then $R(0)p(\nu) = i\tau_0\theta_k p(\nu)$. By using (4.4),(4.5), (4.14) and the definition of $R(0)$, it follows that,

$$\tau_0 \begin{pmatrix} i\theta_k - A_0 & -x_1 & 0 & 0 \\ a_{21} & i\theta_k - a_{22} & 0 & -\eta y_1 \\ -a_{31} & 0 & i\theta_k - a_{22} & 0 \\ 0 & 0 & -b & i\theta_k + b \end{pmatrix} p(0) = \begin{pmatrix} 0 \\ 0 \\ 0 \\ 0 \end{pmatrix}$$

where, $a_{21} = -\mu_1 y_1 e^{-\lambda\tau_1}, a_{31} = -\mu_2 z_1 e^{-\lambda\tau_2}, a_{22} = -r_1 + \eta g_1 + \mu_1 yx1e^{-\lambda\tau_1}$ and $a_{33} = -r_2 + \mu_2 x_1 e^{-\lambda\tau_2}$ to find α_1 and α_2. Similarly, assume that $p^*(s) = G(1,\rho_1,\rho_2,\rho_3)e^{i\tau_0\theta_k s}$ is eigenvector of R^* corresponding to eigenvalue$-i\tau_0\theta_k$ to find ρ_1, ρ_2 and ρ_3. In order to verify $\langle p^*(s), p(\nu)\rangle = 1$, it is essential to evaluate the expression of G. By using (4.15) G is calculated as follows:

$$\begin{aligned} &\langle p^*(s), p(\nu)\rangle \\ &= \overline{G}((1,\rho_1,\rho_2,\rho_3)(1,\alpha_1,\alpha_2,0)^T - \int_{-\tau_1}^{0}\int_{\xi=0}^{\nu} \overline{G}((1,\rho_1,\rho_2,\rho_3)e^{-i\tau_0\theta_k(\xi-\nu)}\mathrm{d}\zeta(\nu)(1,\alpha_1,\alpha_2,0)^T e^{i\tau_0\theta_k\xi}\mathrm{d}\xi \\ &= \overline{G}\Big[1 + \rho_1\alpha_1 + \rho_2\alpha_2 - \Big\{\rho_1\mu_1\tau_1(y_1+\alpha_2x_1)e^{-i\tau_0\theta_k} + \rho_2\mu_2\tau_2(y_1+\alpha_2x_1)e^{-i\tau_0\theta_k}\Big\}\Big]. \end{aligned}$$

Therefore, we choose
$G^{-1} = 1 + \rho_1\alpha_1 + \rho_2\alpha_2 - [\rho_1\mu_1\tau_1(y_1 + \alpha_2 x_1)e^{-i\tau_0\theta_k} + \rho_2\mu_2\tau_2(y_1 + \alpha_2 x_1)e^{-i\tau_0\theta_k}]$ such that $\langle p^*(s), p(\nu)\rangle = 1$. Now, we need to evaluate the coordinates describing the center manifold $\mathbb{C}_0$. Since $\mu = 0$, assume that x_t be solution of (4.13) at $\mu = 0$. For this, we define,

$$u(t) = \langle p^*, x_t\rangle, \qquad W(t,\nu) = x_t(\nu) - 2Re[u(t)p(\nu) \tag{4.11}$$

By center manifold $\mathbb{C}_0$, we get, $W(t,\nu) = W(u(t), \dot{u}(t), \nu)$, where

$$W(u,\overline{u},\nu) = W_{20}(\nu)\frac{u^2}{2} + W_{11}(\nu)u\overline{u} + W_{02}(\nu)\frac{\overline{u}^2}{2} + W_{30}(\nu)\frac{u^3}{6} + ..., \tag{4.12}$$

u and $\overline{u}$ are the local coordinates for the center manifold $\mathbb{C}_0$ in the direction of p and $\overline{p}^*$. $W(u,\overline{u},\nu)$ will be real if x_t is real. Now our aim is to find only real solutions. Since $\mu = 0$, we get

$$\dot{u}(t) = i\tau_0\theta_k u + \overline{p}^*(0)f(0, W(u,\overline{u},0) + 2Re\{up(\nu)\}) = i\tau_0\theta_k u + \overline{p}^*(0)f_0(u,\overline{u})$$

which can be expressed as $\dot{u}(t) = i\tau_0\theta_k u + h(u,\overline{u})$, where

$$h(u,\overline{u}) = \overline{p}^*(0)f_0(u,\overline{u}) = h_{20}\frac{u^2}{2} + h_{11}u\overline{u} + h_{02}\frac{\overline{u}^2}{2} + h_{21}\frac{u^2\overline{u}}{2} + ... \tag{4.13}$$

Now, it can be obtained from (4.11) and (4.12) that

$$\begin{aligned} x_t(\nu) &= (x_{1t}(\nu), x_{2t}(\nu), x_{3t}(\nu), x_{4t}(\nu)) \\ &= W(t,\nu) + 2Re[u(t)p(\nu) \\ &= W_{20}(\nu)\frac{u^2}{2} + W_{11}(\nu)u\overline{u} + W_{02}(\nu)\frac{\overline{u}^2}{2} + ... + u(1,\alpha_1,\alpha_2,0)^T e^{i\tau_0\theta_k\nu} + \overline{u}(1,\overline{\alpha_1},\overline{\alpha_2},0)^T e^{-i\tau_0\theta_k\nu}. \end{aligned}$$

From the definition of $h(u,\overline{u})$, we get

$$\begin{aligned} h(u,\overline{u}) &= \overline{p^*}(0)f_0(u,\overline{u}) \\ &= \tau_0\overline{G}(1,\overline{\alpha_1},\overline{\alpha_2},0)\begin{pmatrix} -\alpha\beta\psi_1^2(0) - \psi_1(0)\psi_2(0) \\ \eta\psi_2(0)\psi_4(0) + \mu_1\psi_1(-\tau_1)\psi_2(-\tau_1) \\ \mu_2\psi_1(-\tau_2)\psi_3(-\tau_2) \\ 0 \end{pmatrix} \\ &= \tau_0\overline{G}\Big[- \alpha\beta\chi_1^2(0) - \psi_1(0)\psi_2(0) + \overline{\alpha}_1(\eta\psi_2(0)\psi_4(0) + \mu_1\psi_1(-\tau_1)\psi_2(-\tau_1)) + \overline{\alpha}_2\mu_2\psi_1(-\tau_2)\psi_3(-\tau_2)\Big] \\ &= -\alpha\beta[u + \overline{u} + W_{20}^1(0)\frac{u^2}{2} + W_{11}^1(0)u\overline{u} + W_{02}^1\frac{\overline{u}^2}{2} + O(|u,\overline{u}|^3)]^2 \\ &\quad - \Big[\{\alpha_1 u + \overline{\alpha_1\overline{u}} + W_{20}^2(0)\frac{u^2}{2} + W_{11}^2(0)u\overline{u} + W_{02}^2(0)\frac{\overline{u}^2}{2} + O(|u,\overline{u}|^3)]^2\} \\ &\quad \times \{u + \overline{u} + W_{20}^1(0)\frac{u^2}{2} + W_{11}^1(0)u\overline{u} + W_{02}^1(0)\frac{\overline{u}^2}{2} + O(|u,\overline{u}|^3)]^2\Big] \\ &\quad + \overline{\alpha_1}\mu_1\Big[\{ue^{-i\theta_k\tau_1} + \overline{u}e^{i\theta_k\tau_1} + W_{20}^1(-\tau_1)\frac{u^2}{2} + W_{11}^1(-\tau_1)u\overline{u} + W_{02}^1(-\tau_1)\frac{\overline{u}^2}{2} + O(|u,\overline{u}|^3)]^2\} \\ &\quad \times \{u\alpha_1 e^{-i\theta_k\tau_1} + \overline{u}\ \overline{\alpha}_1 e^{i\theta_k\tau_1} + W_{20}^2(-\tau_1)\frac{u^2}{2} + W_{11}^2(-\tau_1)u\overline{u} + W_{02}^2(-\tau_1)\frac{\overline{u}^2}{2} + O(|u,\overline{u}|^3)]^2\}\Big] \end{aligned}$$

$$+\overline{\alpha_2}\mu_2\Big[\{ue^{-i\theta_k\tau_2}+\overline{u}e^{i\theta_k\tau_2}+W_{20}^1(-\tau_2)\frac{u^2}{2}+W_{11}^1(-\tau_2)u\overline{u}+W_{02}^1(-\tau_2)\frac{\overline{u}^2}{2}+O(|u,\overline{u}|^3)]^2\}$$
$$\times\{u\alpha_2e^{-i\theta_k\tau_2}+\overline{u}\ \overline{\alpha}_2e^{i\theta_k\tau_2}+W_{20}^2(-\tau_2)\frac{u^2}{2}+W_{11}^2(-\tau_2)u\overline{u}+W_{02}^2(-\tau_2)\frac{\overline{u}^2}{2}+O(|u,\overline{u}|^3)]^2\}\Big]$$

Comparing with the coefficients of equation (4.13), we have

$$\begin{aligned}
h_{20}&=-\alpha\beta-\alpha_1+\alpha_1\overline{\alpha_1}\mu_1e^{-2i\theta_k\tau_1}+\alpha_2\overline{\alpha_2}\mu_2e^{-2i\theta_k\tau_2}\\
h_{02}&=-\alpha\beta-\alpha_1+\overline{\alpha_1}^2\mu_1e^{2i\theta_k\tau_1}+\overline{\alpha_2}^2\mu_2e^{2i\theta_k\tau_2}\\
h_{11}&=-2\alpha\beta-(1+\overline{\alpha}_1\mu_1)Re(\alpha_1)+\overline{\alpha}_2\mu_2Re(\alpha_2)\\
h_{21}&=-\alpha\beta(2W_{11}^1(0)+W_{11}^1(0))-\{W_{20}^2(0)+2W_{11}^2(0)+\overline{\alpha}_1W_{20}^1(0)+2\alpha_1W_{11}^1(0)\}\\
&\quad+\overline{\alpha_1}\mu_1\Big[2\{W_{11}^2(-\tau_1)+\alpha_1W_{11}^1(-\tau_1)\}e^{-i\theta_k\tau_1}+\{\overline{\alpha}_1W_{20}^1(-\tau_1)+W_{20}^2(-\tau_1)\}e^{i\theta_k\tau_1}\Big]\\
&\quad+\overline{\alpha_2}\mu_2\Big[2\{W_{11}^3(-\tau_2)+\alpha_2W_{11}^1(-\tau_2)\}e^{-i\theta_k\tau_2}+\{\overline{\alpha}_2W_{20}^1(-\tau_2)+W_{20}^3(-\tau_2)\}e^{i\theta_k\tau_2}\Big].
\end{aligned}$$

As the expression for h_{21} contains W_{20} and W_{11}, we need to classify W_{20} and W_{11}. Using (4.13) and (4.16), we obtain

$$\begin{aligned}
\dot{W}=\dot{x}_t-\dot{u}p-\dot{\overline{u}}\ \overline{p}&=\begin{cases}RW-2Re\{\overline{p^*}(0)f_\nu\}, & \text{if } \nu\in[-\tau_1,0)\\ RW-2Re\{\overline{p^*}(0)f_\nu\}+f_0, & \text{if } \nu=0\end{cases}\\
&=RW+N(u,\overline{u},\nu),\text{(say)}
\end{aligned}\tag{4.14}$$

where

$$N(u,\overline{u},\nu)=N_{20}(\nu)\frac{u^2}{2}+N_{11}(\nu)u\overline{u}+N_{02}(\nu)\frac{\overline{u}^2}{2}+\text{.....}\tag{4.15}$$

On the other side, by the center manifold $\mathbb{C}_\curlywedge$ neat at origin, it can be written as $\dot{W}=W_u\overline{u}+W_{\overline{u}}\dot{\overline{u}}$
Putting the corresponding series into (4.14) and after comparing, we have

$$\begin{aligned}
(R-2i\tau_0\theta_k)W_{20}(\nu)&=-N_{20}(\nu)\\
RW_{11}(\nu)&=-N_{11}(\nu)
\end{aligned}\tag{4.16}$$

As $\nu\in[\tau_1,0)$,

$$\begin{aligned}
N(u,\overline{u},\nu)&=-\overline{p^*}(0)f_0p(\nu)-p^*\overline{f_0}\overline{p}(\nu)\\
&=-h(u,\overline{u})p(\nu)-\overline{h}(u,\overline{u})\overline{p}(\nu)
\end{aligned}\tag{4.17}$$

Again comparing the coefficient with (4.15), we get

$$\begin{aligned}
N_{20}&=-h_{20}p(\nu)-\overline{h}_{20}\overline{p}(\nu)\\
N_{11}&=-h_{11}p(\nu)-\overline{h}_{11}\overline{p}(\nu)
\end{aligned}\tag{4.18}$$

Using (4.18) and definition of R, it is obtained that $\dot{W}_{20} = 2i\tau_0\theta_k W_{20}(\nu) + h_{20}p(\nu) + \overline{g}_{02}\overline{p}(\nu)$. Therefore,

$$W_{20}(\nu) = \frac{ih_{20}}{\tau_0\theta_k}p(0)e^{i\tau_0\theta_k\nu} + \frac{i\overline{h}_{02}}{3\tau_0\theta_k}\overline{p}(0)e^{-i\tau_0\theta_k\nu} + V_1e^{2i\tau_0\theta_k\nu} \tag{4.19}$$

Again in the same way, from (4.16) and (4.18), we get

$$W_{11}(\nu) = -\frac{ih_{11}}{\tau_0\theta_k}p(0)e^{i\tau_0\theta_k\nu} + \frac{i\overline{h}_{11}}{3\tau_0\theta_k}\overline{p}(0)e^{-i\tau_0\theta_k\nu} + V_2 \tag{4.20}$$

where, $V_1 = (V_1^1, V_1^2, V_1^3, V_1^4)$ and $V_2 = (V_2^1, V_2^2, V_2^3, V_2^4)$ are constant vectors in $\mathbb{R}^4$.

Now, we need to evaluate an suitable form of constant vectors V_2 and V_2. From definition of R and (4.16), we get

$$\int_{-\tau_{-1}}^{0} \mathrm{d}\zeta(\nu)W_{20}(\nu) = 2i\tau_0\theta_k W_{20}(\nu) - N_{20} \tag{4.21a}$$

$$\int_{-\tau_{-1}}^{0} \mathrm{d}\zeta(\nu)W_{11}(\nu) = -N_{11} \tag{4.21b}$$

Again we use (4.14) to get N_{20} and N_{11} as follows:

$$N_{20}(0) = -h_{20}(0)p(0) - \overline{h}_{20}(0)\overline{p}(0) + 2\tau_0\begin{pmatrix} -\alpha\beta - \alpha_1 \\ \mu_1\alpha_1 e^{-2i\tau_1\theta_k} \\ \mu_2\alpha_2 e^{-2i\tau_2\theta_k} \\ 0 \end{pmatrix} \tag{4.22a}$$

$$N_{11}(0) = -h_{11}p(0) - \overline{h}_{11}\overline{p}(0) + 2\tau_0\begin{pmatrix} -\alpha\beta - Re(\alpha_1) \\ \mu_1 Re\{\alpha_1 e^{-2i\tau_1\theta_k}\} \\ \mu_2 Re\{\alpha_2 e^{-2i\tau_2\theta_k}\} \\ 0 \end{pmatrix}. \tag{4.22b}$$

Substituting (4.19) and (4.21a) into (4.22a), we get

$$2i\tau_0\theta_k - \int_0^{-\tau_1} d\zeta(\nu)V_1 = 2\tau_0(-\alpha\beta - \alpha_1, \mu_1\alpha_1 e^{-2i\tau_1\theta_k}, \mu_2\alpha_2 e^{-2i\tau_2\theta_k}, 0)^T.$$

Hence,

$$\begin{pmatrix} i\theta_k + A_0 & x_1 & 0 & 0 \\ -a_{21} & i\theta_k + a_{22} & 0 & \eta y_1 \\ a_{31} & 0 & i\theta_k + a_{22} & 0 \\ 0 & 0 & b & i\theta_k - b \end{pmatrix} V_1 = 2\begin{pmatrix} -\alpha\beta - \alpha_1 \\ \mu_1\alpha_1 e^{-2i\tau_1\theta_k} \\ \mu_2\alpha_2 e^{-2i\tau_2\theta_k} \\ 0 \end{pmatrix}.$$

Using Crammer's rule, $V_1^1, V_1^2, V_1^3, V_1^4$ can be obtained. Again, substituting (4.20) and (4.21b) into (4.22b), we have

$$-\int_0^{-\tau_1} \mathrm{d}\zeta(\nu)V_2 = 2\tau_0(-\alpha\beta - Re(\alpha_1), \mu_1 Re\{\alpha_1 e^{-2i\tau_1\theta_k}\}, \mu_2 Re\{\alpha_2 e^{-2i\tau_2\theta_k}\}, 0)^T.$$

Hence,

$$\begin{pmatrix} -A_0 & -x_1 & 0 & 0 \\ a_{21} & -a_{22} & 0 & -\eta y_1 \\ -a_{31} & 0 & -a_{22} & 0 \\ 0 & 0 & -b & b \end{pmatrix} V_2 = 2\begin{pmatrix} -\alpha\beta - Re(\alpha_1) \\ \mu_1 Re\{\alpha_1 e^{-2i\tau_1\theta_k}\} \\ \mu_2 Re\{\alpha_2 e^{-2i\tau_2\theta_k}\} \\ 0 \end{pmatrix}.$$

Similarly, $V_2^1, V_2^2, V_2^3, V_2^4$ can also be evaluated by Crammer's rule.

Thus, we get h_{21} using $W_{20}(\nu)$ and $W_{11}(\nu)$ from (4.19) and (4.20) respectively. Therefore, we can evaluate the following values

$$\begin{aligned}
\varrho(0) &= \frac{i}{2\tau_0\theta_k}\left(h_{11}h_{20} - 2|h_{11}|^2 - \frac{|h_{02}|^2}{3}\right) + \frac{h_{21}}{2},\\
\kappa_1 &= -\frac{Re\{\varrho(0)\}}{Re\{\lambda'(0)\}},\\
\kappa_2 &= 2Re\{\varrho(0)\},\\
T_2 &= -\frac{Im\{\varrho(0)\} + \kappa_1 Im\{\lambda'(0)\}}{\tau_0\theta_k}.
\end{aligned} \tag{4.23}$$

Here, κ_1 indicates the direction of Hopf-bifurcation, κ_2 indicates the stability of Hopf-bifurcating periodic solution and T_2 represents periodic solution at critical value $\tau = \tau_k^j$. By the center manifold theorem and results of Hassard *et al.*, the properties of Hopf-bifurcation can be summarised as a theorem.

Theorem 4.1. *If the following results hold [26] in expression (4.23) then,*

i) there is subcritical or supercritical Hopf-bifurcation if $\kappa_1 < 0$ or $\kappa_1 > 0$,
ii) there is unstable or stable bifurcating periodic solutions if $\kappa_2 < 0$ or $\kappa_2 > 0$,
iii) the period of bifurcating solutions decrease or increase if $T_2 < 0$ or $T_2 > 0$.

5. Numerical simulations and biological implications

In this section, we present the numerical results of the model system to study the effect of immune-activation distributed delay, discrete delays and different parameters. The parameter values given in Table 1 have been used to obtain numerical simulations. For parameter values $b = 4, \mu_1 = 0.04, \mu_2 = 0.015$ and $\eta = 0.0375$, the tumor free equilibrium and tumor presence equilibrium are obtained as $E_0(0, 1.02509, 6.90909, 6.90909)$ and $E_1(0.362843, 1.63481, 7.66788, 7.66788)$ respectively. After a few calculations, we have $\eta_0 \simeq 0.1743$ and $\eta_1 \simeq 0.0437$. From Theorem 3.3, it can be noted that the tumor-free equilibrium is asymptotically stable for $0.0437 < \eta < 0.1743$. Using Theorem 4.1, the values of κ_1, κ_2 and T_2 can be evaluated. From explicit expressions (4.23) and given parameter values, one can calculate $\kappa_1 = 59.6107(> 0), \kappa_2 = -2.5379(< 0)$ and $T_2 = 2.1523(> 0)$. As $\kappa_1 > 0$ and $\kappa_2 < 0$, the Hopf bifurcation is supercritical and the bifurcating periodic solution is stable and its period increases (as $T_2 > 0$) when τ_1 crosses the critical value τ_1^* from left to right.

5.1. Influence of μ_1: Stimulation rate of ECs in presence of TCs

Figure 2a–f captures the effect of the stimulation rate μ_1 of effector cells (ECs) in presence of tumor cells (TCs) on the dynamics of tumor-immune interaction. For $\mu_1 = 0.038$ and $\tau_1 = 0.2$ days $< \tau_1^*$ (bifurcation point) $= 0.282$ days $= 6.768$ h, the system shows an unstable equilibrium with a regular periodic behavior to tumor presence equilibrium point E_1. This implies that expansion of tumor cells in immunizing process is under host-defensive as well as tumor-enhancement actions of immunity [7]. As the value of μ_1 increases, the system exhibits a change from unstable to stable regime. Figure 2d–f shows stable dynamics of the system at $\mu_1 = 0.05$ and $\tau_1 = 0.2$ days $= 4.8$ h. The system admits Hopf bifurcation at μ_1^* (critical point) $= 0.045$ for $\tau_1 = 0.2$ days (Fig. 7a–c) and sustains periodic oscillation. With increasing μ_1, the amplitude of periodic oscillation for tumor cells changes to a damped oscillatory solution. Ultimately, the effector cells and helper T cells are capable of lysing tumor cells. At this stage tumor cells are non-invasive [28].

TABLE 1. Parameter values for numerical simulations.

Dimensional parameter	Value	Dimensionless parameter	Value
a (the intrinsic growth rate of tumor cells)	0.431day^{-1} [30]	α	1.636
m (the carrying capacity of tumor cells)	2×10^{-9}cells [30]	β	0.002
s_1 (constant flow of effector cells)	1.3×10^{4} cells [30]	ω_1	0.1181
d_1 (loss of effector cells)	$0.412\,\text{day}^{-1}$ [30]	r_1	0.3743
s_2 (constant flow of helper T cells)	$(0.02-0.2)\,\text{h}^{-1}$ [21]	ω_2	0.38
d_2 (loss of helper T cells)	$(0.1277-0.6456)\,\text{s}^{-1}$ [21]	r_2	0.055

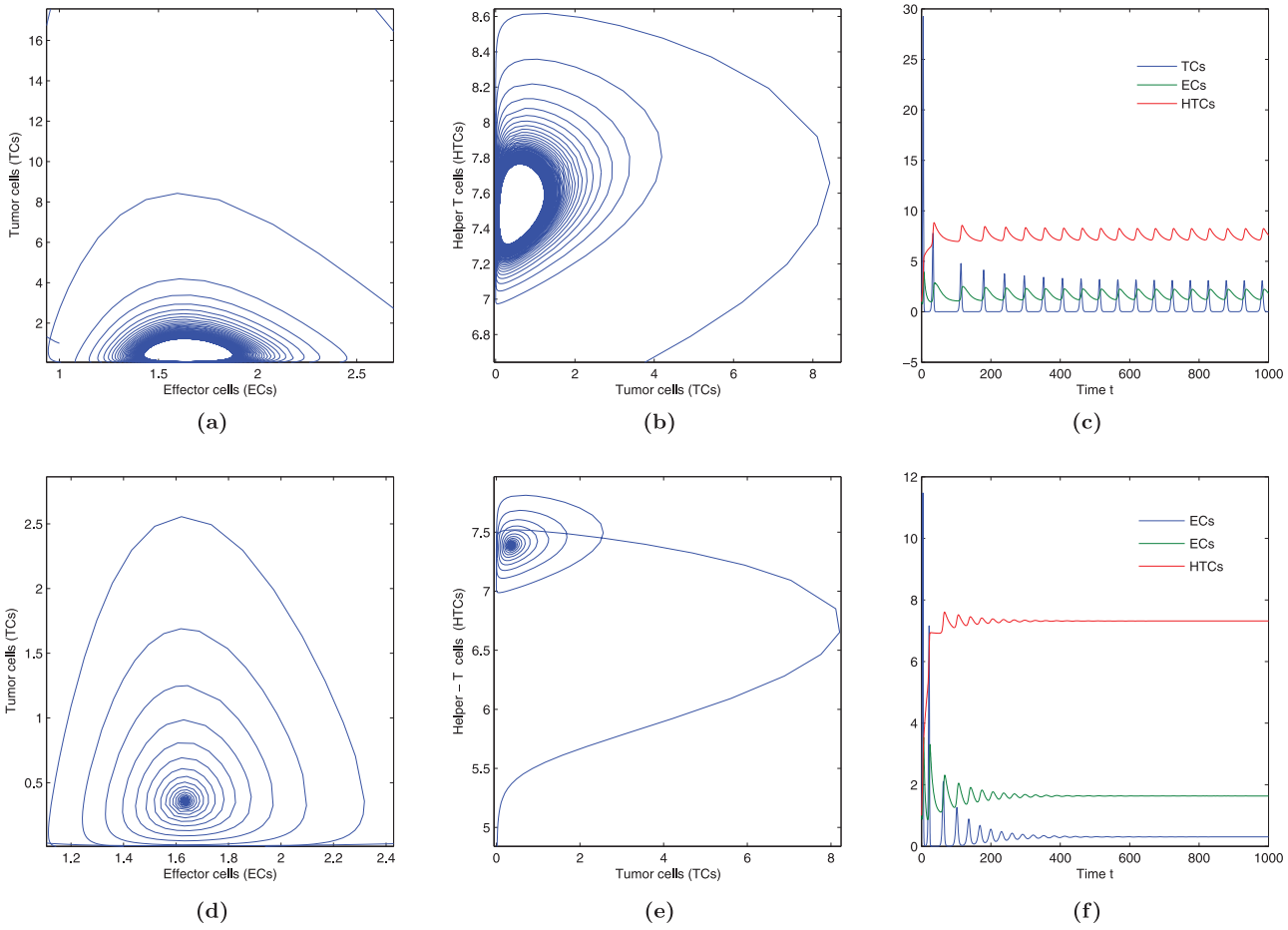

FIGURE 2. (a,b) show the phase portrait diagram of TCs-ECs, TCs-HTCs and (c) shows time evaluation curve of system for $\mu_1 = 0.038, \tau_1 = 0.2$ days $= 4.8$ h. (d,e) present the phase portrait diagram of TCs-ECs, TCs-HTCs and (f) presents time evaluation curve of system for $\mu_1 = 0.05, \tau_1 = 0.2$ days $= 4.8$ h.

5.2. Influence of μ_2: Stimulation rate of HTCs in presence of TCs

Figure 3a–f illustrates how the dynamics of tumor-immune interaction depends on the stimulation rate μ_2 of helper T cells (HTCs)in presence of tumor cells(TCs). For $\mu_2 = 0.215$ and $\tau_2 = 0.25$ days $= 6$ h, the system approaches a steady state with damping oscillatory behavior(Fig. 3c). With increasing μ_2, the system undergoes

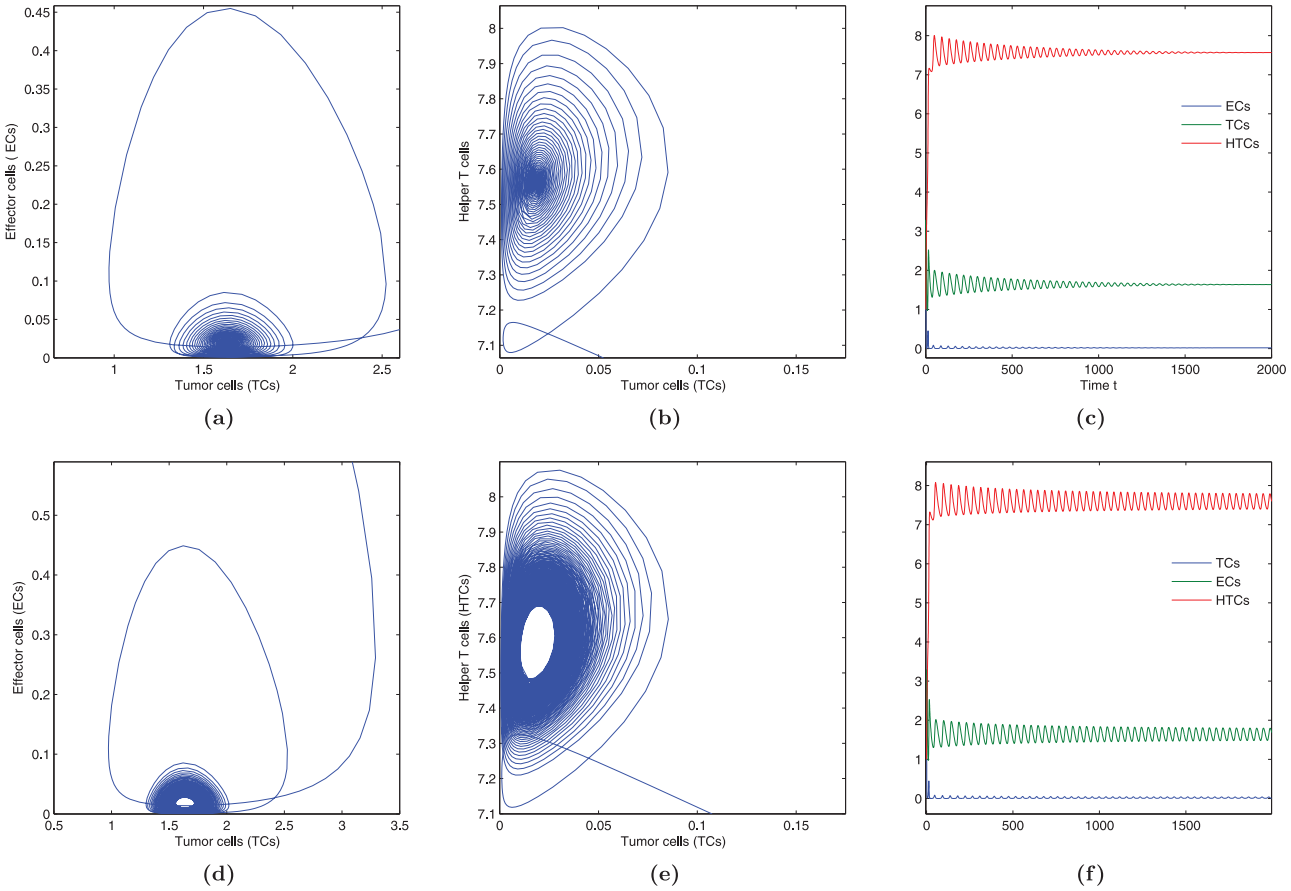

FIGURE 3. (a,b) present the phase portrait diagram of TCs-ECs, TCs-HTCs and (c) shows time evaluation curve of system for $\mu_2 = 0.215, \tau_2 = 0.25$ days $= 6$ h. (d,e) present the phase portrait of TCs-ECs, TCs-HTCs and (f) presents time evaluation of system for $\mu_2 = 0.28$, $\tau_2 = 0.25$ days $= 6$ h.

a change in stability property and a small amplitude of periodic oscillation is demonstrated. Thus the system exhibits a Hopf bifurcation at μ_2^* (bifurcation point) $= 0.223$ (Fig. 8a–c). Finally, beyond Hopf threshold, a stable oscillation is observed with very low amplitude governing the persistent oscillatory behavior of tumor cells that may be mentioned as dormancy [23, 30].

5.3. Influence of τ_1: Interaction delay between ECs and TCs

The dynamics of tumor-immune interaction due to change in discrete time delay τ_1 is observed in Figure 4a–f. For $\tau_1 = 0.21$ days $< \tau_1^*$ (bifurcation point) $= 0.282$ days and $b = 4$, the system shows stable equilibrium (Fig. 4c) and approaches the tumor presence equilibrium E_1 with a damping oscillatory behavior. As τ_1 increases, the system experiences a changing dynamics from stability to instability. At $\tau_1 = 0.282$ days $= 6.768$ h, a Hopf-bifurcation is observed (Fig. 9a) in the system. Consequently high amplitude of periodic oscillation is observed (Fig. 4f) as τ_1 increases. This means that the 'patient's situation' is in advance stage due to increase of interaction time delay τ_1, which corresponds to metastatic state [31].

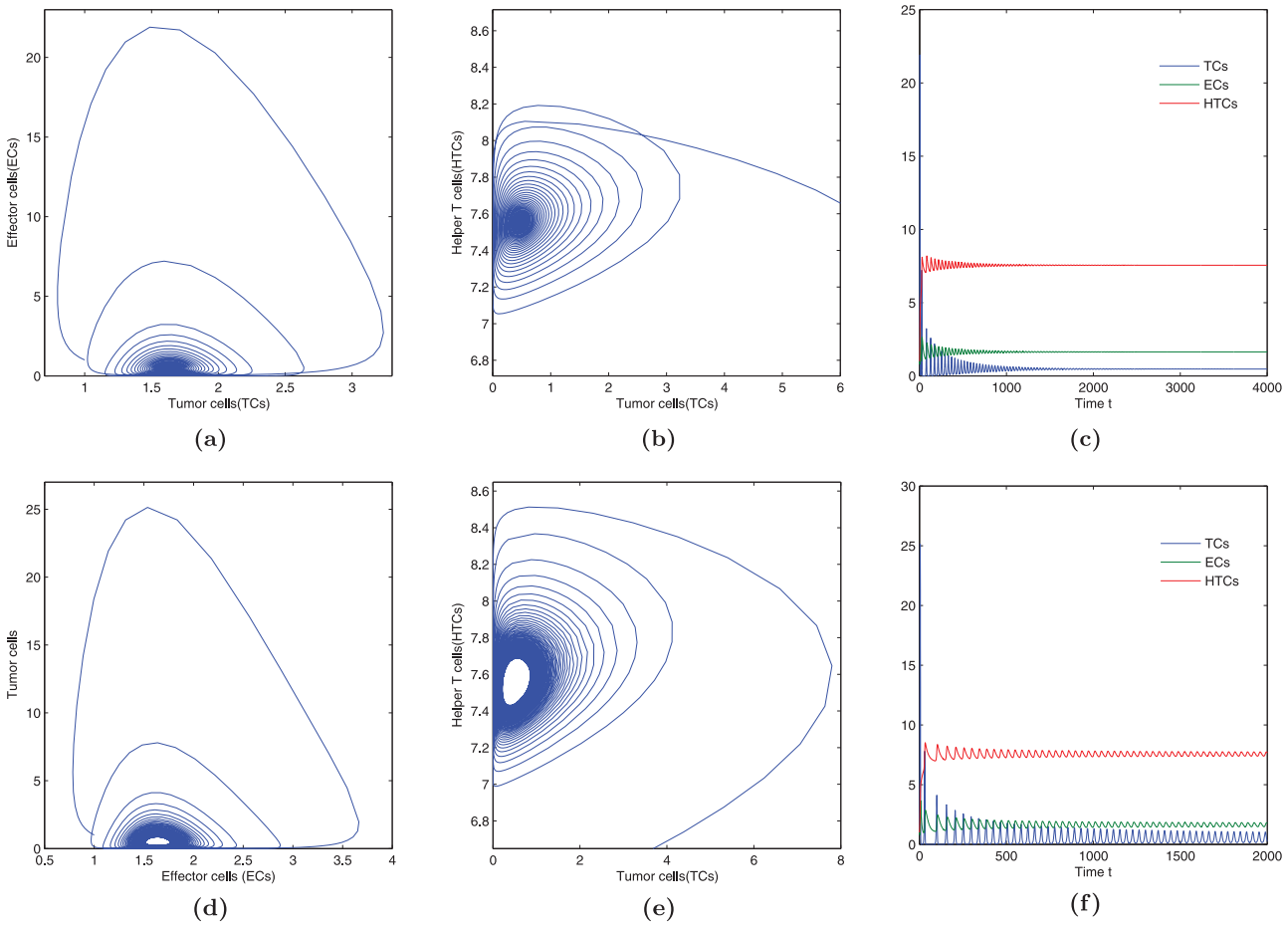

FIGURE 4. (a,b) show the phase portrait diagram of TCs-ECs, TCs-HTCs and (c) shows time evaluation curve of system for $\tau_1 = 0.21$ days $= 5.04$ h, $b = 4$. (d,e) present the phase portrait diagram of TCs-ECs, TCs-HTCs and (f) presents time evaluation curve of system for $\tau_1 = 0.33$ days $= 7.92$ h, $b = 4$.

5.4. Influence of τ_2: Maturation delay between HTCs and TCs

Figure 5a–d show the effect of maturation delay τ_2 on the dynamics of tumor-immune interaction. For $\tau_2 = 5$ days and $b = 4$, a very small periodic oscillatory behavior at steady-state value E_1 is observed in Figure 5a which is dormant state of tumor. It can be observed in Figure 5b that the immune system can control tumor burden for a short time. As τ_2 increases, a quasi-periodic behavior has flourished as the system shows rare and irregular long periodic oscillations. This means a long delay in immune response may develop the tumor to more incursive state [7]. Also further increase of τ_2, there occurs a stability switch (Fig. 5c), the system shows unstable behavior leading to quasi-periodic phenomena. This indicates that tumor growth is beyond controlled. As a result, tumor cells are highly dependent on healthy tissue cells.

5.5. Influence of b: The strength of immune-activation delay of HTCs

5.5.1. Influence of b when $\tau_1 > 0$ and $\tau_2 = 0$

Figure 6a–d illustrate how the strength of distributed delay, b can change the dynamics in presence of interaction delay τ_1. For $b = 0.18 < b^*$ (bifurcation point) $= 0.218$ and $\mu_1 = 0.35$, a stable damping oscillatory

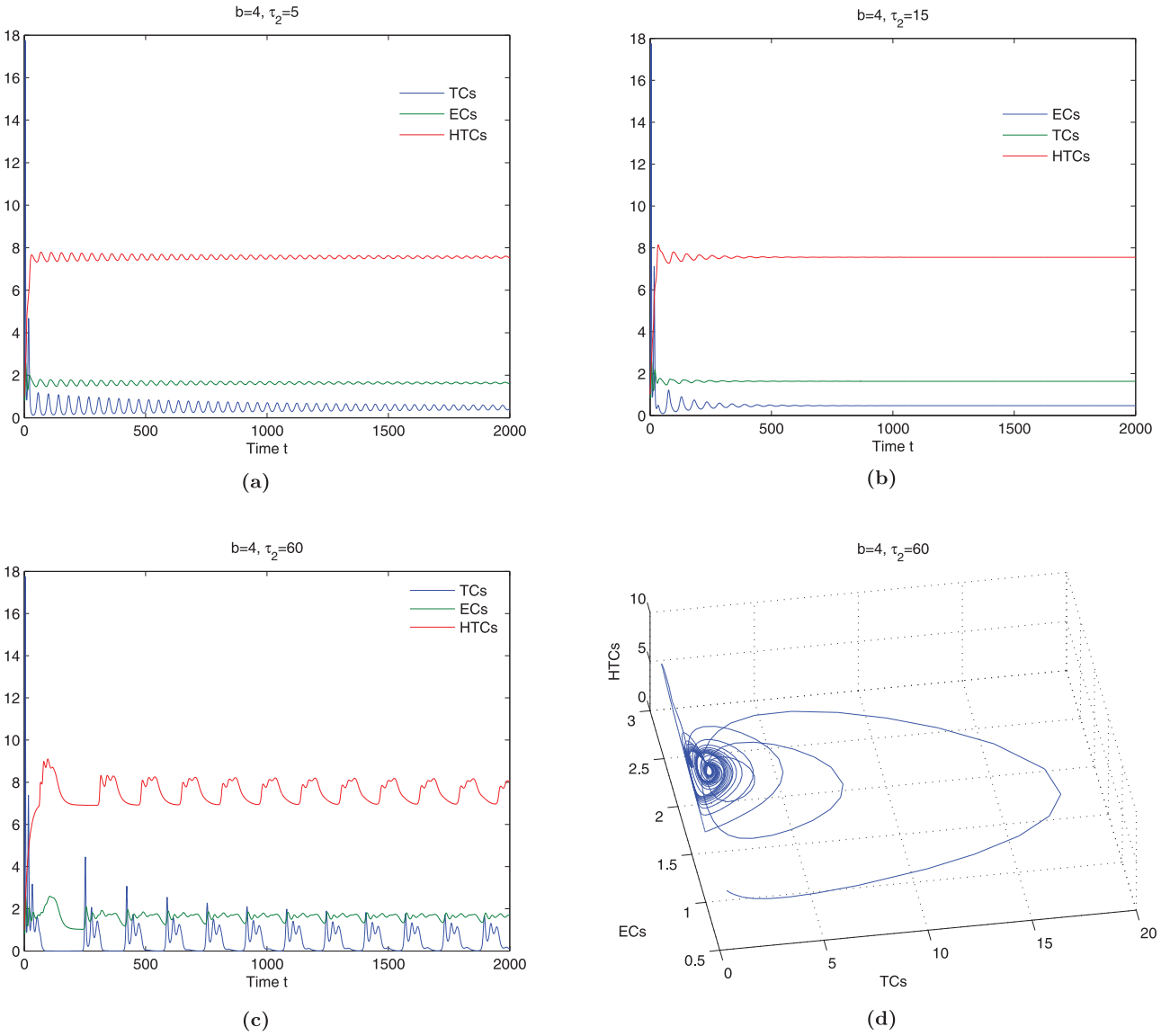

FIGURE 5. (a–c) present time evaluation curve of system for (a) $\tau_2 = 5$ days $= 120$ h, $b = 4$, (b) $\tau_2 = 15$ days, $b = 4$ and (c) $\tau_2 = 60$ days, $b = 4$, (d) presents the three-dimensional quasi-periodic phase portrait diagram for $\tau_2 = 60$ days.

behavior of the system of tumor presence equilibrium E_1 is observed. As the value of b increases, the oscillation of tumor cells decreases after some recovery time(Fig. 6b). For $\tau_1 = 0.35$ days $= 8.4$ h, the system exhibits Hopf-bifurcation at $b = 0.218$. With increasing b, the amplitude of oscillation tumor cells increase for tumor cells (Fig. 6d) and there is a change in dynamics from damped oscillations to periodic oscillation, *i.e.*, effector cells and helper T cells do not have any impact on tumor cells.

5.5.2. Influence of b when $\tau_2 > 0$ and $\tau_1 = 0$

Similar to Section **5.6.2**, changing dynamics due to variation in b in presence of maturation delay, τ_2 are illustrated in Figure 7a–d. For $b = 0.2$, $\tau_2 = 4$ days, the system shows stable behavior. As value of b increases,

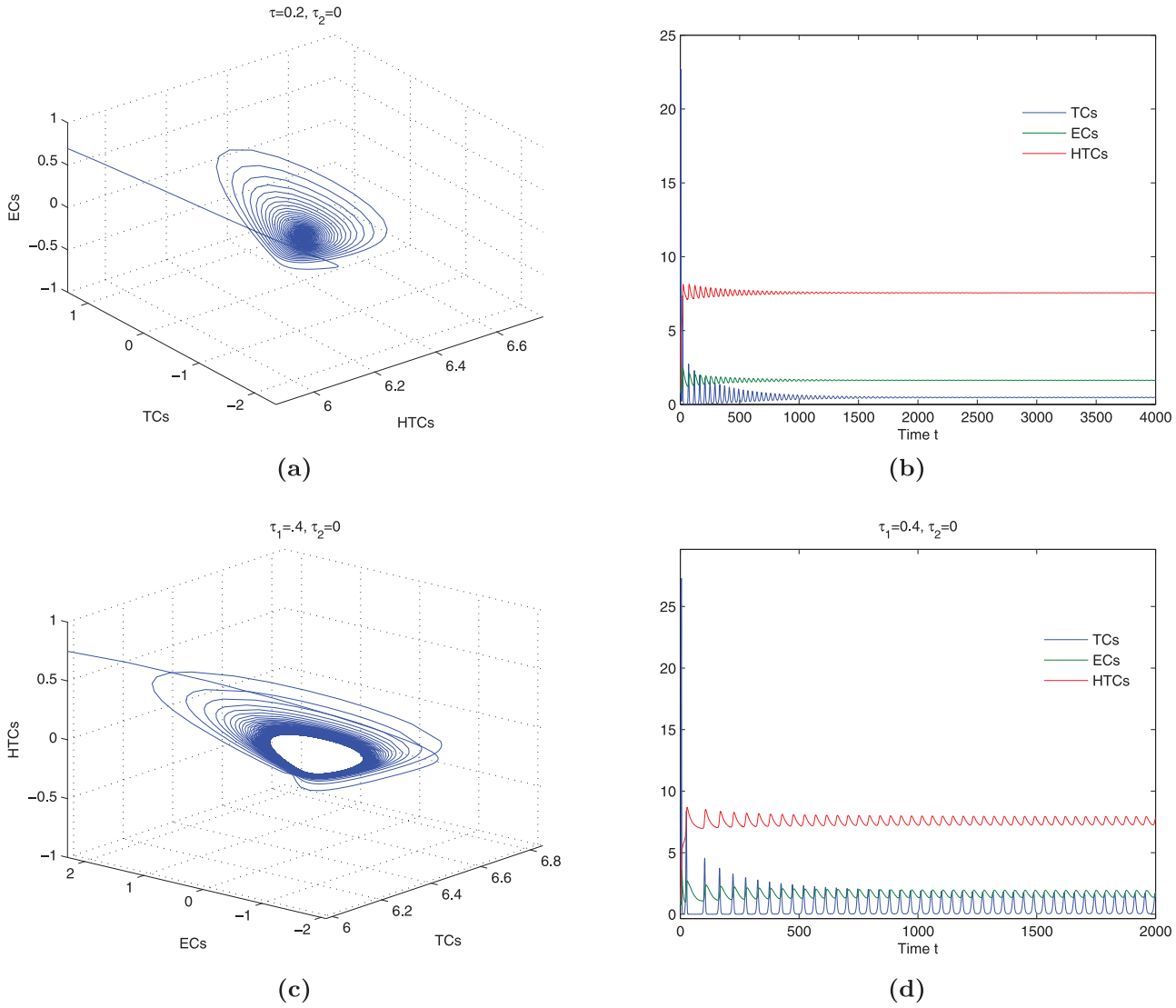

FIGURE 6. (a) and (c) show the three dimensional phase portrait diagram for (a) b = 0.15 and (c) b = 0.31 with $\tau_1 = 0.2$ days = 4.8 h. (b) and (d) present the time evaluation curve of system for (b) b = 0.15 and (d) b = 0.31 with $\tau_1 = 0.2$ days = 4.8 h.

the system undergoes bifurcation at b^* (critical point) = 0.23. For $b = 0.3$ and $\tau_2 = 4$ days, periodic oscillations of tumor cells with large amplitude are shown in Figure 7d. As a result, the tumor burden increases beyond the critical value of $b = 0.23$. At this stage, tumor state is invasive.

5.6. Bifurcation analysis

The analysis of Hopf-bifurcation is more important in the dynamics of tumor-immune interaction due to the occurrence of limit cycle around the critical point and resulting stable and unstable periodic solutions. The periodic solutions provide the clinical symptoms of tumor dynamics as it indicates the oscillation of tumor growth levels around the equilibrium point due to lack of any kind of treatments. Now, our aim is to investigate

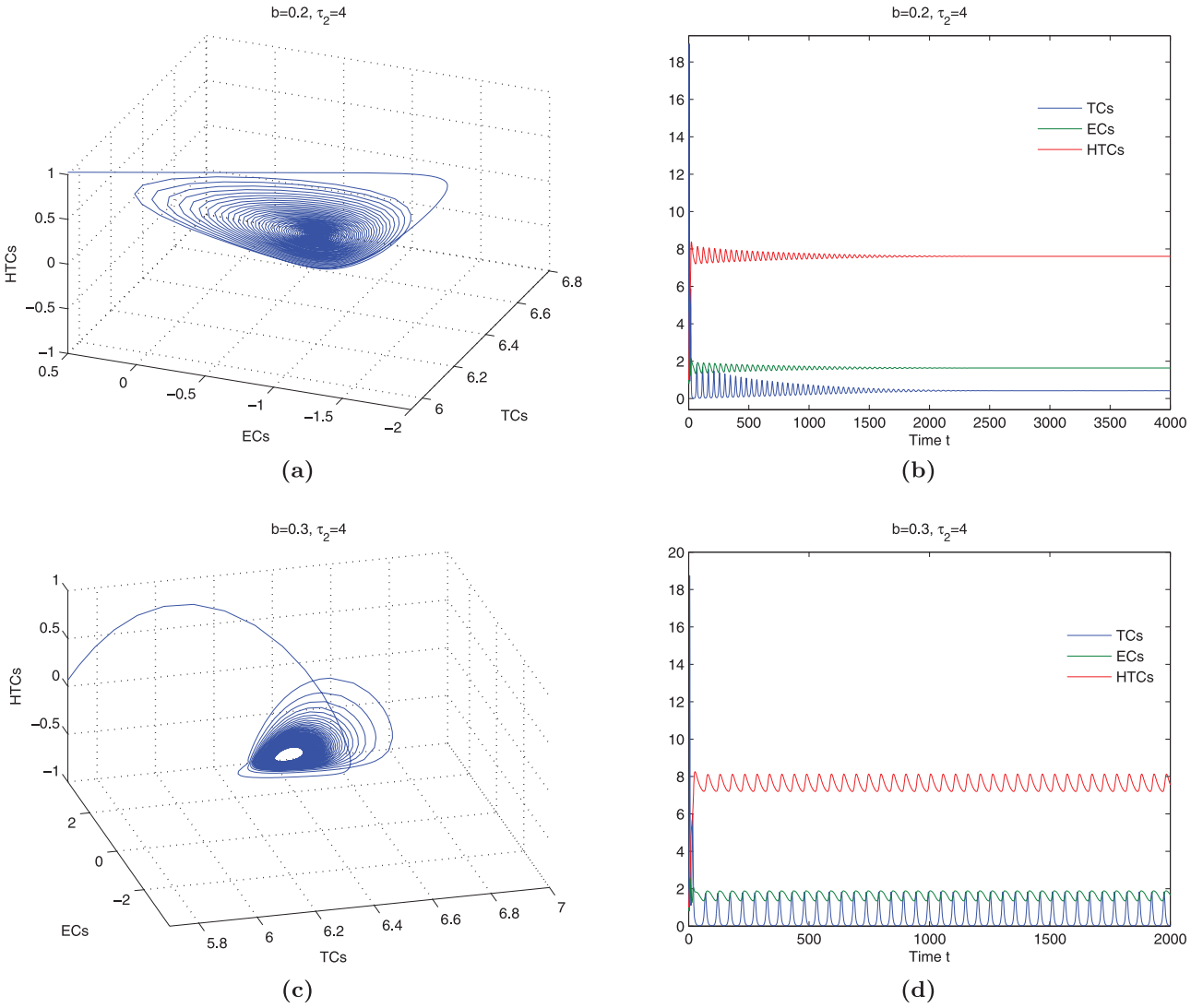

FIGURE 7. (a) and (c) show the three dimensional phase portrait diagram for (a) b = 0.18 and (c) b = 0.35 with $\tau_2 = 4$ days. (b) and (d) present the time evaluation curve of system for (b) b = 0.18 and (d) b = 0.35 with $\tau_2 = 4$ days.

the different situations for which we change the parameter values. Here $\mu_1, \mu_2, \tau_1, \tau_2$ and b are bifurcating parameters and remaining parameter values are given in Table 1.

5.6.1. Bifurcation diagram for μ_1

Figure 8a–c shows the bifurcation of the system with respect to μ_1, the stimulation rate of effector cells (ECs) in presence of tumor cells (TCs). Below the threshold value μ_1^* (bifurcation point) = 0.045, the tumor cells are in the unstable state. Beyond the Hopf threshold, the population of tumor cells, effector cells and helper T cells gradually reduce the periodicity. Finally, the system reaches a stable steady state. This implies that the stimulation rate does not affect the system in range $\mu_1 > \mu_1^* = 0.045$, *i.e.*, tumor growth doesn't depend on μ_1 whenever $\mu_1 > \mu_1^*$.

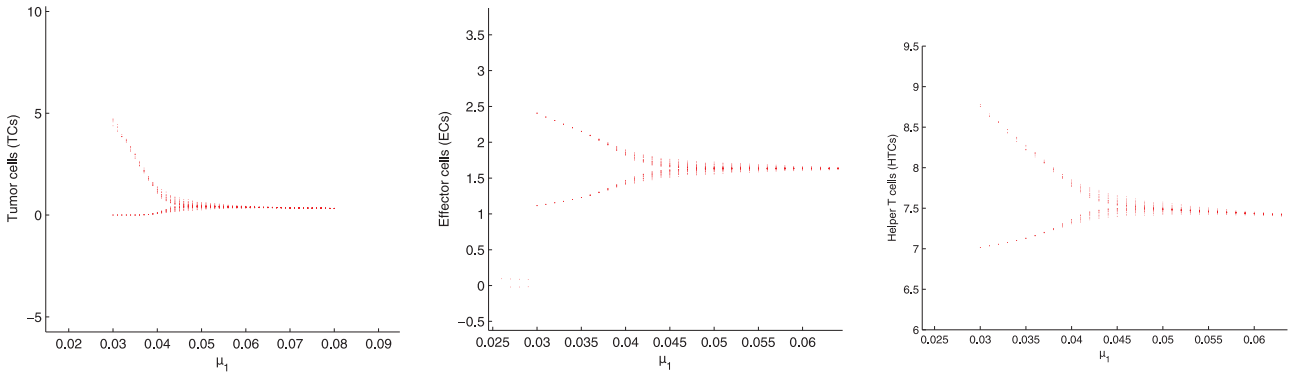

FIGURE 8. Bifurcation diagrams of the tumor-immune system (2.2) for $\mu_1 \in (0, 0.08)$, (a) μ_1 *versus* TCs, (b) μ_1 *versus* ECs and (c) μ_1 *versus* HTCs with other parameter values given in Table 1.

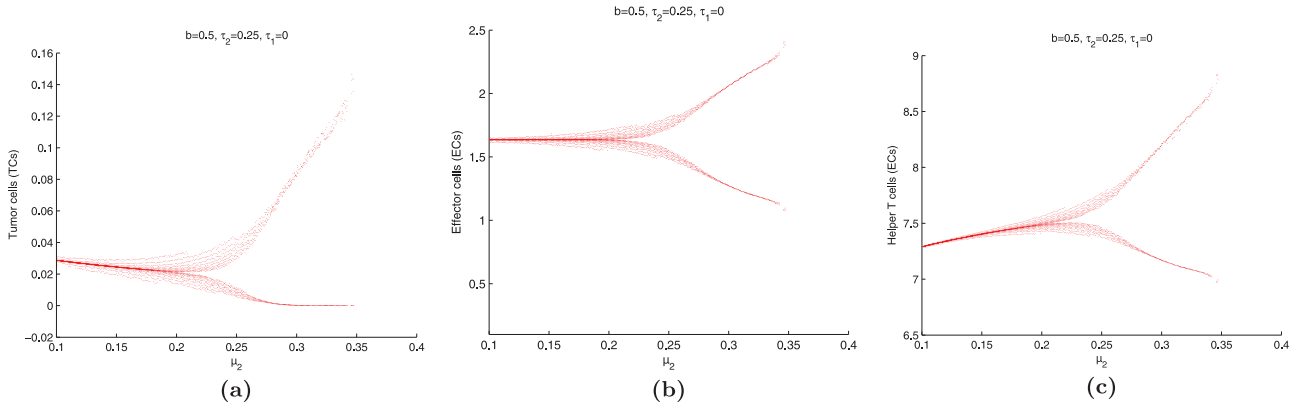

FIGURE 9. Bifurcation diagrams of the tumor-immune system (2.2) for $\mu_2 \in (0, 0.4)$, (a) μ_2 *versus* TCs, (b) μ_2 *versus* ECs and (c) μ_2 *versus* HTCs with other parameter values given in Table 1.

5.6.2. Bifurcation diagram for μ_2

Figure 9a–c illustrates the Hopf bifurcation of the system with respect to the proliferation rate μ_2 of helper T cells (HTCs) in presence of tumor cells (TCs) and effector cell (ECs). In the range $0 < \mu_2 < \mu_2^*$ (bifurcation point) $= 0.223$, the tumor cells are controlled by effector cells and helper T cells and a stable limit cycles exists. Beyond the critical value $\mu_2^* = 0.223$, the growth of tumor cells highly depends on μ_2.

5.6.3. Bifurcation diagram for τ_1

Figure 10a shows the Hopf-bifurcation of the system with respect to interaction delay τ_1. In the range $0 < \tau_1 < \tau_1^*$ (bifurcation point) $= 0.282$ days $= 6.768$ h, the system shows the stable steady state of tumor presence equilibrium point E_1 and this implies that the density of tumor cells is well controlled by ECs and HTCs. At this stage tumor characteristic is non-metastatic and dormant. Beyond the critical value τ_1^*, the tumor cells exhibit stable oscillator behavior with higher amplitude. This implies that the growth of tumor cells depend on τ_1.

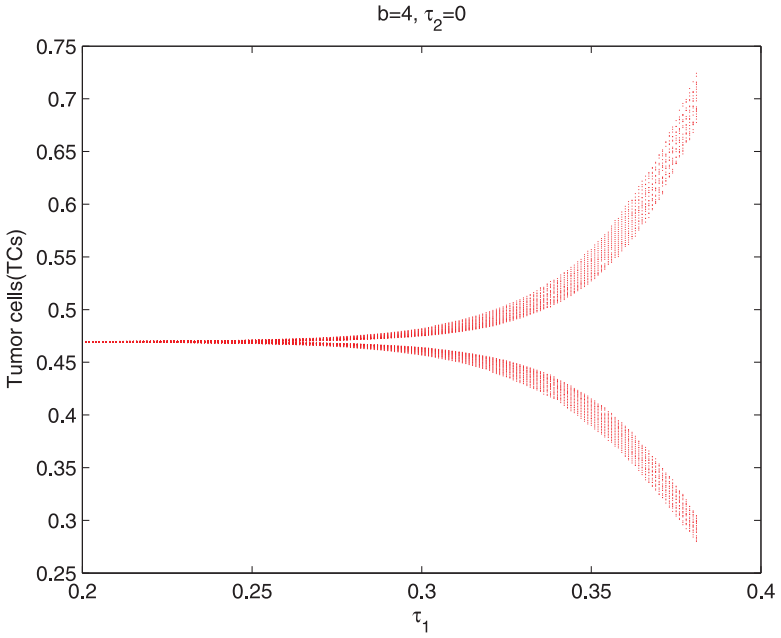

FIGURE 10. Bifurcation diagram of the system with respect to τ_1 with $\tau_1^* = 0.282$.

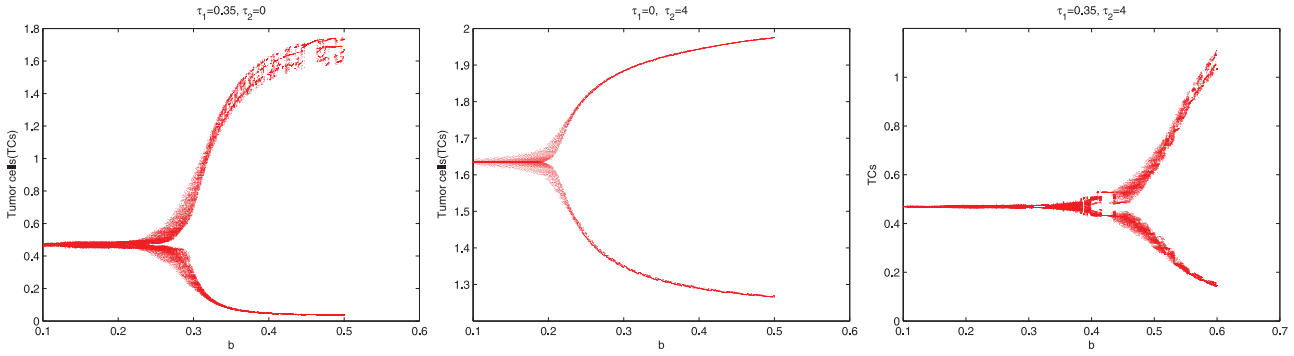

(a) (b) (c)

FIGURE 11. Bifurcation diagrams of the tumor-immune system (2.2) for $b \in (0, 0.6)$, (a) b *versus* tumor cells with $\tau_1 = 0.35$ days $= 8.4$ h, (b) b *versus* tumor cells with $\tau_2 = 4$ days $= 96$ h (c) b *versus* tumor cells with $\tau_1 = 0.35$ days $= 8.4$ h and $\tau_2 = 4$ days $= 96$ h. Rest of parameter values defined in Table 1.

5.6.4. Bifurcation diagram for b

Figure 11a demonstrates Hopf-bifurcation with respect to b, the strength of distributed delay in presence of interaction delay τ_1. The stability of the system changes around the critical value $b^*_{\tau_1}$ (bifurcation point in presence of τ_1) $= 0.218$. Below the threshold value, the system shows damped oscillations with stable limit cycles of tumor presence equilibrium E_1. Beyond the critical value $b^*_{\tau_1}$, tumor cells show a regular periodic oscillation. Similarly in Figure 11a, the system admits Hopf-bifurcation with respect to b around $b^*_{\tau_2}$ (bifurcation point in presence of τ_2) $= 0.23$ in presence of maturation delay τ_2 in Figure 11b. It is observed that the immune activation is highly dependent on the population of helper-T cells (HTCs). At time t, the larger value of b shows

weak delay effect while the smaller value of b at past time $t - v$ may demonstrate strong delay effect. Figure 11c illustrates Hopf-bifurcation diagram. The system shows stable steady state of tumor presence equilibrium with increase of b, strength of immune activation delay in presence of discrete time delays. At $b^*_{\tau_1\tau_2}$ (bifurcation point in presence of τ_1 and τ_2) = 0.361, Hopf-bifurcation has occurred. Furthermore, it can be noticed that stability regime for parameter b is relatively larger than that of any discrete delay. This implies that uniformly activated HTCs help in ECs stimulation and also controls tumor burden simultaneously.

6. Concluding remarks

Nowadays it is more essential to consider natural phenomena by introducing time delays in the demonstration of tumor-immune interaction. A simple mathematical model can play an important role to interpret the nature of a tumor-immune dynamics and help to reveal better treatment technique. Indeed, it may be challenging to deal with experimental studies to trace real delay patterns in T-IS interplay where our present work can give some important insights.

In the previous study [17], the existing tumor-immune interaction model considered the discrete delays between tumor cell– effector cell and tumor cell–helper T cell. Then the dynamics have also been investigated in the presence of delays. However, the activation delays can even stabilize the immune-control equilibrium. But current study reveals that the activation of a helper-T cell is not an instantaneous process. Helper-T cells become activated by interaction with an antigen-presenting cell such as macrophages. After this, the activated HTCs stimulate the immune-effector cell. Due to these reasons, in this research, we have incorporated a continuous delay kernel in HTCs to illustrate the inner scenarios of tumor- immune interaction. Our analytical findings are well complemented with numerical simulations. Here, we have demonstrated positivity of the solutions, boundedness of the system and investigated local stability by Routh-Hurwitz criterion. The qualitative analysis of Hopf-bifurcation with respect to different parameters has been studied. The direction of Hopf-bifurcation and the stability of bifurcating periodic solution based on center manifold theorem has been derived explicitly. While observing the dynamics, the influence of the immune activation delay along with discrete delays has been highlighted. For understanding complex biological scenarios, we have analyzed numerical simulations to validate the analytical findings. It is observed that beyond the Hopf-threshold, our model generates periodic oscillation which is biologically appropriate and realistic as similar kind of dynamics are observed in cancer patients. Moreover, few simulations exhibit that increase of delays may cause a change from stable to unstable dynamics. Otherwise, local stability allows the tumor to reach near values for their carrying capacity(maximum tumor size). As stability switch has occurred in the system, this phenomena interprets that immune system receives the message of oscillatory tumor growth. As a result, the immune system becomes more effective to annihilate tumor cells. But, for excessive delay in immune interaction, the immune system becomes less effective to control tumor growth.

In the beginning, we have observed that effector cells are able to control tumor growth for stimulation rate $\mu_1 > 0.045$. Similarly, if stimulation rate μ_2 of helper-T cells crosses critical value $\mu_2^* = 0.045$, the tumor becomes invasive. Also, interaction delay τ_1 plays a key role, the tumor is beyond the control of effector cells if $\tau_1 > \tau_1^*$ (= 0.282 days = 6.768 h) *i.e.*. it takes more time to stimulate effector cells to initiate annihilation of tumor cells. Hence, the parameters μ_1 and μ_2 play a key role to boost HTCs and ECs in controlling tumor burden.

We have investigated the influence of immune activation delay strength b. It has been discussed that the immune response is a continuous process. So if we increase the strength of distributed delay, the immune response can be increased equivalently. We have observed that tumor is stable in presence of τ_1 for below critical value $b^*_{\tau_1} = 0.218$ days = 5.232 h and similarly in presence of τ_2, tumor is stable for below $b^*_{\tau_2} = 0.230$ days = 5.52 h. But for below of $b^*_{\tau_1\tau_2} = 0.361$ days = 8.664 hours, the system remains stable for larger time. Nevertheless, distributed delay along with discrete delays play a crucial role for the larger stability regime of tumor growth than any individual delay or both delays (Fig. 11a–c). Again we have taken $\tau_1 > 0$ and $\tau_2 = 0$ for tumor angiogenesis. There exists Hopf-threshold value for τ_1 crossing which unstable steady state is manifested due to longer delay. This implies a larger interaction delay couldn't affect the tumor burden. Here "*Sneaking*

through" phenomena are observed [30], which refers low doses of tumor cells fail to mount an effective tumor-immune response and gradually tumor grows, similarly medium doses of tumor cells lead to tumor eradication and large doses develop tumor cells through immune defenses.

However, it has been observed that the stability regime for b, the strength of continuous delay is relatively larger than that of the presence of any delay. From a qualitative point of view, a set of parameter values have been derived which may design new diagnostic and control technique to interrupt tumor growth. This assures that the uniformly activated helper-T cells help in the stimulation of ECs and also control the tumor burden simultaneously which indicates the applicability of our proposed research. We would like to deepen our analysis of the study of $CD8^+$ T cells and tumor cells in the future.

Acknowledgements. The authors thank to the Editor Dr. Vitaly Volpert and the anonymous referees who provided insightful comments and valuable suggestions for better exposition of the manuscript. Parthasakha Das is supported by Indian Institute of Engineering Science and Technology, Shibpur, under institute fellowship.

References

[1] Society AC. Cancer Facts & figures 2019. American Cancer Society, Atlanta, 2019.
[2] J. Adam and N. Bellomo, A Survey of Models for Tumor Immune Dynamics. Birkhauser, Boston (1997).
[3] R.P. Araujo and D.L.S. McElwain, A history of the study of solid tumor growth: the contribution of mathematical modelling. *Bull. Math. Biol.* **66** (2004) 1039–1091.
[4] S. Banerjee and S.S. Sarkar, Delay-induced model for tumor-immune interaction and control of malignant tumor growth. *BioSystems* **91** (2008) 268–288.
[5] J.J. Batzel and K. Kappel, Time delay in physiological systems: Analyzing and modeling its impact. *Math Biosci.* **234** (2011) 61–74.
[6] P. Bi and S. Ruan, Bifurcations in delay differential equations and applications to tumor and immune system interaction models. *SIAM J. Appl. Dyn. Syst.* **12** (2013) 1847–1888.
[7] P. Bi, S. Ruan and S. Zhang, Periodic and chaotic oscillations in a tumor and immune system interaction model with three delays. *Chaos* **24** (2014) 023101.
[8] G. Caravagna and A. Graudenzi, Distributed delays in a hybrid model of tumor-immune system interplay. *Math. Biosci. Eng.* **10** (2013) 37–57.
[9] E. Coddington and N. Levinso Theory of ordinary differential equation. McGraw-Hill, New Delhi (1955).
[10] M. Cohn, *Int. Immunol.* **20** (2008) 1107–1118.
[11] K.L. Cooke and Z. Grossman, Discrete Delay, Distributed Delay and Stability Switches. *J Math. Anal. Appl.* **86** (1982) 592–627.
[12] P.S. Das, P. Das and A. Kundu, Delayed feedback controller based finite time synchronization of discontinuous neural networks with mixed time-varying delays. *Neural Process Lett.* **49** (2018) 693–709.
[13] P.S. Das, P. Das and S. Das, An investigation on Monod–Haldane immune response based tumor–effector–interleukin–2 interactions with treatments. *Appl. Math. Comput.* **361** (2019) 536–551.
[14] P.S. Das, S. Mukherjee and P. Das, An investigation on Michaelis-Menten kinetics based complex dynamics of tumor-immune interaction. *Chaos Soliton Fractals* **128** (2019) 197–305.
[15] P.S. Das, P. Das and S. Mukherjee, Stochastic dynamics of Michaelis-Menten kinetics based tumor-immune interactions. *Physica A* **541** (2020) 123603.
[16] L. De Pillis and A. Radunskaya, A mathemtical model with immune resistance and drug therapy: an optimal control approach. *J. Thor. Med.* **3** (2001) 79–100.
[17] Y. Dong, R. Miyazaki and Y. Takeuchi, Mathematical modelling on helper T-cells in a tumor immune system. *Discrete Contin. Dyn. Syst.* **19** (2014) 55–72.
[18] Y. Dong, G. Huang, R. Miyazaki and Y. Takeuchi. Dynamics in a tumor immune system with time delays. *Appl. Math. Compt.* **252** (2015) 99–113.
[19] A. D'Onofrioa, F. Gatti, P. Cerrai and L. Freschi, Delay-induced oscillatory dynamics of tumor-immune system interaction. *Math. Comput. Model.* **51** (2010) 572–591.
[20] C.W. Eurich, A. Thiel and L. Fahse, Distributed Delays Stabilize Ecological Feedback Systems. *Phys. Rev. Lett.* **94** (2005) 158104.
[21] S. Feyissa and S. Banerjee, Delay-induced oscillatory dynamics in humoral mediated immune response with two time delays. *Nonlinear Anal. Real World Appl.* **14** (2013) 35–52.
[22] U. Forys, Stability and bifurcations for the chronic state in Marchuk's model of an immune system. *J Math. Anal. Appl.* **352** (2009) 922–942.
[23] M. Galach, Dynamics of tumor-immune system comptition-the effect of the time delay. *Int. J. Math. Comput. Sci.* **13** (2003) 395–406.
[24] D. Ghosh, S. Khajanchi, S. Mangiarotti, F. Denis, S.K. Dana and C. Letellier, How tumor growth can be influenced by delayed interactions between cancer cells and the microenvironment? *BioSystems* **157** (2017) 17–30.

[25] J.K. Hale and S.M.A. Lunel, Introduction to functional Differential Equations. Springer-Verlag, New York (1993).
[26] B.D. Hassard, N.D. Kazarinoff and Y.H. Wan, Theory and Application of Hopf Bifurcation. University of Cambridge, Cambridge (1981).
[27] S. Khanjanchi, Bifurcation analysis of a delayed mathematical model for tumor growth. *Chaos Solitons Fractals* **77** (2015) 264–276.
[28] S. Khajanchi and S. Banerjee, Stability and bifurcation analysis of delay induced tumor immune interaction model. *Appl. Math. Comput.* **248** (2014) 652–671.
[29] D.E. Kirschner and J.C. Panetta, Modelling the immunotheraphy of tumor-immune interaction. *J. Math. Biol.* **37** (1998) 235–252.
[30] V.A. Kuznetsov, I.A. Makalkin, M.A. Taylor and A.S. Perelson, Non-linear dynamics of immunogenic tumors: parameter estimation and global bifurcation analysis. *Bull. Math. Biol.* **56** (1994) 295–321.
[31] H. Mayer, K. Zaenker and U. Heiden, A basic mathematical model of the immune response. *Chaos* **5** (1995) 155–161.
[32] M.J. Piotrowska and M. Bodnar, Influence of distributed delays on the dynamics of a generalized immune system cancerous cells interactions model. *Commun. Nonlinear Sci. Numer. Simul.* 54 (2018) 379–415.
[33] M.J. Piotrowska, M. Bodnar, J. Poleszczuk and U. Forys, Mathematical modelling of immune reaction against gliomas: sensivity analysis and influence of delays. *Nonlinear Anal. Real World Appl.* **14** (2013) 1601–1620.
[34] F.A. Rihan, D.H.A. Rahaman, S. Lakshmanan and A.S. Alkhajeh, A time delay model of tumor-immune system interactions: global dynamics, parameter estimation, sentivity analysis. *Appl. Math. Comput.* **232** (2014) 606–623.
[35] S. Ruan and J. Wei, On the zeros of transcendental functions with applications to stability of delay differential equations with two delays. *Dyn. Contin. Discret. Impuls Syst. Ser A* **10** (2003) 863–874.
[36] M. Villasana and A. Radunskaya A delay differential equation model for tumor-growth. *J. Math. Biol.* **47** (2003) 270–294.
[37] X. Yang, L. Chen and J. Cheng, Parmanance and positive periodic solution for single-species non-autonomous delay diffusive model. *Comput. Math. Appl.* **32** (1996) 109.
[38] M. Yu, Y. Dong and Y. Takeuchi, Dual role of delay effects in a tumour- immune system. *J Biol. Dyn.* **11** (2017) 334–347.